Ore Geology Reviews 57 (2014) 29–52

Contents lists available at ScienceDirect

Ore Geology Reviews

journal homepage: www.elsevier.com/locate/oregeorev

Titaniferous heavy mineral aggregates as a tool in exploration for pegmatitic and aplitic rare-metal deposits (SE Germany)

Harald G. Dill [a,*], Berthold Weber [b], Frank Melcher [a], Werner Wiesner [c], Axel Müller [d]

[a] Federal Institute for Geosciences and Natural Resources, P.O. Box 510163 D-30631 Hannover, Germany
[b] Bürgermeister-Knorr Str. 8 D-92637 Weiden i.d.OPf., Germany
[c] Armanspergstraße 4, D-94505 Bernried, Germany
[d] Geological Survey of Norway, Leiv Eirikssons vei 39, N-7491 Trondheim, Norway

ARTICLE INFO

Article history:
Received 10 April 2013
Received in revised form 20 August 2013
Accepted 27 August 2013
Available online 8 September 2013

Keywords:
Heavy mineral aggregates
Titanium
Rare metals
Pegmatites
Drainage system
SE Germany

ABSTRACT

Black heavy mineral (HM) aggregates of metallic luster and composed of ilmenite and rutile were named "nigrine" (amount of rutile > ilmenite) and "antinigrine" (amount of ilmenite > rutile). They contain inclusions of, e.g., columbite-(Fe), pyrochlore group minerals, wolframite solid solution series (= s.s.s.), monazite, zircon, Fe oxides and sulfides as well as alteration minerals such as pseudorutile and Fe–Ti–Nb–Ta–Al–P compounds, whose precise chemical composition and mineralogical affiliation cannot be determined. These titaniferous HM aggregates are of widespread occurrence in gneisses and shear zones cutting through them as well as alluvial, fluvial and colluvial deposits at different distances from rare-element phosphate pegmatites within the crystalline basement in SE Germany. "Nigrine" and "antinigrine" may be subdivided into three types which formed at different periods relative to the Variscan tectonic disturbances and which show different qualities as markers for the origin and presence of Nb-bearing pegmatites along the western edge of the Bohemian Massif, SE Germany.
Type A developed pre- to synkinematically within or near deep-seated shear zones which formed below 730 °C as early as 321 to 329 Ma. These HM aggregates are poor in Nb and impoverished in accessory minerals. The HM aggregates having developed in shear zones mark the "kitchen" where friction and heating contributed to the formation of felsic intrusive bodies, such as pegmatites and aplites. This type of Ti-bearing HM aggregates may be held as distal proximity indicator.
Type B is early postkinematic and enriched in niobian rutile, rife with lots of inclusions, especially columbite-(Fe). It precipitated in the crystalline country rocks at temperatures around 600 °C concomitant with the nearby rare-element pegmatites between 302 and 311 Ma. It is the most proximal member of this group of HM aggregates.
Type C "nigrine" is enriched in W and late postkinematic relative to the shearing processes in the crystalline basement. It formed around 470 °C during the same period of time as type C. It does, however, not qualify as a marker for rare-element pegmatites, as it is unrelated to these felsic intrusives.
During the late Neogene the Variscan basement was strongly uplifted and many pegmatites were stripped off their roof rocks. As a consequence of this, "nigrine" and "antinigrine" were released from their host rocks and became part of the terrigenous sediments laid down in the drainage systems which upstream cut into the crystalline basement and the pegmatites/aplites. Due to their high resistance to chemical weathering these titaniferous HM aggregates acted as "armored relics" for less resistant minerals such as columbite and pyrochlore. When these titaniferous HM aggregates got decomposed by attrition these mineral inclusions of lesser stability appear in the fluvial sediments further afield from their source than expected, considering the low stability to weathering of single crystals of columbite- and pyrochlore group minerals.
"Antinigrine" and "nigrine" may be spotted in the HM suites of drainage systems around pegmatites at a distance of ≤10 km with correlation coefficient of $R_{Nb-Ti} = +0.42$, while in the range 2–5 km R_{Nb-Ti} increases to +0.77, in the range 1–2 km R_{Nb-Ti} is +0.85 and around 1 km from the rare-element pegmatite R_{Nb-Ti} stands at +0.92.
"Nigrine" and "antinigrine" are no ideal mineral aggregates to form placer-type deposits of their own due to their variegated mineralogy, excluding some Ta-enriched subtypes in Colombia and Sierra Leone. The variable mineralogy detrimental to its use as a source of Ti, is the strong point as an exploration tool for rare-element pegmatites.

1. Introduction

Geochemical methods are widely used in mineral exploration and may considerably contribute to the search of new mineral deposits.

* Corresponding author. Tel.: +49 511 643 2361.
E-mail address: dill@bgr.de (H.G. Dill).
URL: http://www.hgeodill.de (H.G. Dill).

0169-1368/$ – see front matter © 2013 Elsevier B.V. All rights reserved.
http://dx.doi.org/10.1016/j.oregeorev.2013.08.023

Consequently, several textbooks or text-book-like comprehensive papers have been published on this key discipline (Fletcher, 1997; Komov et al., 1994; Levinson, 1974; Peters, 1987; Zhovinsky, 1993). Even if the most suitable sampling media (plants, sediments, water) and the most highly sophisticated analytical techniques have been selected and given the data of the survey have been correctly interpreted, forward modeling of the target area based on chemistry as a stand-alone method is rather limited. To fill in this gap and supplement the chemical techniques in applied economic geology, the study of the physical/mechanical dispersion around ore deposits has been considered as a valuable tool in exploration. The resultant stream sediments containing minerals and lithoclasts can be checked for diagnostic heavy minerals (abbreviated to HM and introduced in the Abstract) which may assist in drawing a picture of the primary deposit much better than using chemical exploration as a stand-alone method (Duk-Rodkin et al., 2001; Hou et al., 2008; Lalomov and Bochneva, 2008; Morton, 1991; Siegfried, 2008). The HM may be encountered at different sites from the alluvial deposits through the coastal environment of deposition. A broadening of the data base may be achieved, when HM aggregates of the same sort of minerals, such as complex penetration twins of cassiterite or mineral aggregates derived from intergrowth of different but genetically related mineral species are concerned (Dill et al., 2006). The latter type of HM aggregates dominated by different Ti minerals is the centerpiece of the current investigation. Titanium minerals intimately intergrown with each other are host to mineral inclusions, they provide vugs and notches to take up sediments during the process of transport and deposition and they are widely distributed in the drainage systems intersecting crystalline basement rocks which were intruded by granites, pegmatites as well as aplites (Dill et al., 2008a,b).

Apart from the dominant alkaline feldspar, albite, muscovite and quartz, LCT- (Li–Cs–Ta) or NYF (Nb–Y–F)-pegmatites contain a variegated spectrum of minerals, very widespread in the pegmatites proper, but rather seldom found among the HM of stream sediments (Abella et al., 1995; Anderson et al., 1998; Černý, 1989, 2005; Ercit, 2005; London, 2005; Novák et al., 2003; Sweetapple and Collins, 2002; Wise, 1999). The NE Bavarian Basement contains both rock types, it is rife with pegmatites and aplites and its sediments on top and in the foreland are abundant in HM aggregates, called "nigrine" and "antinigrine", closely related to these felsic intrusives (Figs. 1, 2).

A tripartite approach has been taken to study HM aggregates in view of both, genetic and applied geosciences.

Firstly, the scope of the current study is to present a sort of HM aggregates made up predominantly of oxidic Ti minerals, as to its outward appearance and its sedimentological traps so as to help their recognition in the field and ease its application as an exploration tool.

Secondly, the studies in the laboratory under the scanning electron microscope (SEM) and electron probe microanalyzer (EPMA) aimed at defining the most diagnostic mineralogical and textural parameters for a precise determination of the origin of their pegmatitic/aplitic source rocks. In terms of exploration, it is meant to define types of HM aggregates indicative of basement areas fertile for pegmatites and those crustal sections which are of lithological relevance but less likely an economic target.

Thirdly, alteration of these HM aggregates was studied as a tool to constrain the physical–chemical regime along transport and deposition of the HM during the Cenozoic.

Since these mineral aggregates have not attracted much attention during the recent past and the term "nigrine" is not very well entrenched in geosciences, its discovery and definition is briefly reported prior to the presentation of our results. Titanium was discovered by William Gregor in 1791 in ilmenite and recognized as a new element by the German chemist Klaproth in 1791 when studying rutile. Prior to the discovery of Ti, "nigrine" was confounded for cassiterite whose penetration twins closely resemble these HM aggregates with regard to its hardness and when abraded to its outward appearance (Walravens, 2006). G. A. Werner, attracted by the deep black color (in the classical language Latin, "niger" means black), proposed the name "nigrine" for what he believed to be a new mineral (Stütz, 1799). It was not until 1860 that Rammelsberg cast doubt on the quality of previous chemical analyses and stated that "nigrine" has to be considered as an intergrowth of rutile and ilmenite (Rammelsberg, 1860). The definition which our studies are based upon comes close to what has been put forward by Ramdohr (1975): "Nigrine" is a mineral aggregate of ilmenite and rutile, displaying a black metallic luster. Both minerals are intergrown with each other in various textural types and the resulting aggregates may bear mineral inclusions and/or alteration minerals.

In the present study we make an amendment as to the quantity of the major components in the build-up of this mineral aggregate, following the well-known naming of an intergrowth of albite and orthoclase whose types of intergrowth are well entrenched in the literature as "perthite" and "anti-perthite". In the current situation, if rutile is the dominant phase the result is named "nigrine" and vice versa, if ilmenite prevails over rutile it is called "antinigrine".

2. Methodology

In the Northeast Bavarian Basement and its foreland 120 samples have been taken from creeks and small rivers in the NE Bavarian Basement, SE Germany, from outcrop of crystalline rocks in the basement and at rivers draining its immediate foreland (Fig. 1). The data obtained by the various methods formed the basis for the list of chemical and mineralogical data presented in Table 1.

The loose to semi-consolidated stream sediments were subjected to granulometric studies in the laboratory. The particle size of the clastic rocks under consideration was determined in the classical way by sieving and by means of a CAMSIZER for grain size and morphological analyses. The CAMSIZER® measuring system is based on digital image processing. The bulk material flow falls between a light source and a high-resolution digital camera. All particles are optically recorded when passing by its lens as to their grain size, digitized and processed in the connected computer. The data are denoted in the common way in terms of sphericity and roundness values, using the schemes and comparison charts elaborated by Illenberger (1991) and Tucker (2001) for grain morphology.

The data obtained throughout these laboratory investigations were plotted in the conventional way as cumulative frequency curves using a mm scale along the x-axis. The quartiles Q_1 (25%), Q_2 (50%) and Q_3 (75%) formed the basis to calculate the Trask's parameters median grain size (Md) and sorting coefficients.

Prior to the HM analysis the samples were sieved and the grain size fraction 63 to 600 μm was used for follow-up HM separation. During routine analyses, the HM (density >2.9 g/cm^3) were extracted by means of Na-polywolframate. After removal of iron oxide coatings with Na dithionite, translucent HM plus LM were mounted on glass disks using Canada balsam and identified under the petrographic microscope, considering between 200 and 300 grains per sample for mineral analysis.

The gravel-sized HM fragments was hand-picked, because it was unable to pass through the sieve and together with samples from the hard rock were investigated by means of EPMA and the scanning electron microscope equipped with energy-dispersive X-ray system (SEM-EDX).

The EPMA was used to determine the chemical composition of mineral aggregates and the accessory minerals. Electron microprobe analyses were carried out using a CAMECA SX100 equipped with five wavelength dispersive spectrometers and a Princeton Gamma Tech energy-dispersive system. Oxide and silicate phases were analyzed at 20 kV acceleration voltage and 20 nA sample current (on brass). Counting times were 10 s on peak and 5 s on each background. The following X-ray lines, spectrometer crystals and standards (in brackets) were used: Na Kα, TAP (albite); Mg Kα, TAP (chromite, kaersutite); Al Kα, TAP (chromite, almandine); Si Kα, TAP (rhodonite, almandine); P Kα, PET (apatite); S Kα, PET (pentlandite); K Kα, PET (biotite); Ca Kα,

PET (apatite, kaersutite); Sc Kα, PET (metal); Ti Kα, LLIF (rutile, kaersutite); V Kα, LLIF (metal); Cr Kα, LLIF (chromite); Mn Kα, LLIF (rhodonite); Fe Kα, LLIF (magnetite, almandine); Ni Kα, LLIF (metal); As Lα, TAP (AsGa); Nb Lα, PET (metal); Sn Lα, PET (metal); Ta Lα, LIF (metal); W Lα, LLIF (metal); Pb Mα, PET (PbS); and U Mα, PET (metal).

For SEM investigation a FEI Quanta 600F operated in low-vacuum mode (0.6 mbar) was used. Therefore, sputtering of the samples with gold or carbon is not necessary. The microscope is equipped with the EDX-system Genesis 4000 of EDAX.

XRD patterns were recorded using a PANalytical X'Pert PRO MPD Θ-Θ diffractometer (Cu-Kα radiation generated at 40 kV and 30 mA), equipped with a variable divergence slit (20 mm irradiated length), primary and secondary Soller collimator, scientific X'Celerator detector (active length 0.59°), and a sample changer (sample diameter 28 mm). The samples were scanned from 2° to 90° 2Θ with a step size of 0.0167° 2Θ and a measuring time of 20 s per step. For specimen preparation the top loading technique was used. XRD was used for aliquots of the bulk sample to get an overview of the amount of rutile and ilmenite in the concentrate.

The chemical composition of the concentrates was determined using a PANalytical Axios and a PW2400 spectrometer. Samples were prepared by mixing with a flux material (Lithium metaborate Spectroflux, Flux No. 100A, Alfa Aesar) and melting into glass beads. The beads were analyzed by wavelength dispersive X-ray fluorescence spectrometry (WD-XRF). To determine loss on ignition (LOI) 1000 mg of sample material was heated to 1030 °C for 10 min.

Concentrations of Li, Be, B, Al, P, K, Rb, Sr, Sb, Zn, Ga, Ti, Mn, Fe, and Ge in quartz from shear zones were analyzed in situ by laser-ablation inductively-coupled plasma mass spectrometry (LA-ICP-MS). More details of the analytical procedure are provided by Flem et al. (2002).

3. Geological setting

The oldest crystalline rocks, gneisses of different mineralogical composition, are found in the SE part of the study area, in the Bayerischer and Böhmer Wald, along the western edge of the Bohemian Massif (Fig. 1b, c). They are of Upper Proterozoic age (Franke, 1989; Weber and Vollbrecht, 1986). These pre-Variscan basement rocks, the core zone of the central European Variscides, form part of the Moldanubian zone (Moldanubicum) at the north-Gondwana margin and were subdivided into the Monotonous and Varied Groups (Von Raumer et al., 2003). It is representative of the autochthonous unit (Fig. 1c). The paragneisses have been derived from greywackes and arenites. They are intercalated with amphibolites of magmatic derivation (Dill, 1989).

On this autochthonous unit the Bohemicum, a coherent allochthonous nappe was thrusted. Today this structural unit is split up by the erosion into different klippens (erosional remnants of the former coherent nappe) such as the region between Teplá-Domažlice in the Czech Republic, the Zone of Erbendorf-Vohenstrauß (ZEV) and the northernmost part the Münchberg Gneiss Complex (MM) in Fig. 1c. The MM is interpreted as a tectonic klippe resting upon low to medium grade metamorphic Paleozoic and Upper Proterozoic rocks of the Saxothuringian zone (Saxothuringicum) that occupy much of the central part of the study area in the NE Bavarian Basement.

Towards the NW un-metamorphosed sedimentary and volcanic rocks of Middle Cambrian through Early Carboniferous age developed. Late stages of Variscan convergence in mid-Carboniferous times resulted in the deformation and folding of these afore-mentioned rocks and the emplacement of synorogenic granites (Seltmann and Faragher, 1994). It has to be noted that the region under consideration is intersected by deep-seated lineamentary fault zones of different size and length. The most prominent one is the NW–SE striking Great Bavarian Quartz Lode ("Pfahl") spawning some NNW–SSE striking offshoots along its southern rim (Fig. 1b). Smaller quartz lodes and several swarms of quartz veins such as at the western edge of the Hagendorf–Pleystein pegmatite province are not shown on this map for reasons of scale.

The Late Paleozoic quartz veins and granites were accompanied by pegmatitic and aplitic rocks enriched in Li, Nb and P, the latter giving rise to a variable association of phosphate minerals, some of which are enriched in Li and Sc, as well as columbite- and pyrochlore group minerals (Dill et al., 2007a,b, 2008b, 2011, 2012a) (Fig. 1b).

During the Upper Carboniferous and Permian, a basin-and range topography evolved in the uplifted Variscan orogen, with narrow basins subsiding in the crystalline basement rocks and collecting the debris of the Proterozoic and early Paleozoic basement rocks around that underwent erosion. Continental and marine sequences made up of clastic rocks alternating with calcareous and evaporitic beds were deposited during the Triassic, followed by a marine transgression during the Jurassic leaving behind a vast carbonate platform (Fig. 1b).

During the Cenozoic the basement and its foreland were subjected to another pervasive chemical weathering resulting in large kaolin deposits and were pierced by basaltic necks. A low-relief landscape in the basement evolved during the Neogene under subtropical climates (Borger et al., 1993). During the Quaternary fluvial incision gave rise to the present-day drainage systems and alluvial–fluvial deposits which host the HM aggregates under consideration.

4. Results

4.1. The outward appearance of HM aggregates and their sedimentary traps

4.1.1. Morphology and grain size

The Ti-bearing aggregates may easily be identified in the field by their black metallic luster and high specific gravity which oscillates around 4.5 g/cm^3, dependent upon the amount of rutile (specific gravity 4.25 g/cm^3) and ilmenite (specific gravity 4.72 g/cm^3) present in the HM aggregate (Fig. 2a). The roundness and morphology of sediments attaining cobble- to gravel size were described with the naked eye, and when dealing with arenaceous stream sediments, determined under the scanning electron microscope or using the CAMSIZER. Common schemes and comparison charts such as those designed by Pettijohn et al. (1973), Illenberger (1991) and Tucker (2001) have proven to be a valuable tool for comparison.

The grain morphology is highly variable and spans the interval from rounded to subangular, the grain shape runs the gamut from rods to almost isometric spheres in loose and semi-consolidated sediments (Fig. 2a, b). In the "nigrine–antinigrine" host rocks, in quartz veins and gneissic rocks, the angularity of rutile–ilmenite intergrowth falls in the roundness class "angular" (Fig. 2c). The HM aggregates from the Pflaumbach fluvial deposits near Pleystein in the Hagendorf–Pleystein pegmatite province show a rather good sorting (Fig. 2d). A typical grain size analysis of arenaceous stream sediments abundant in Ti-bearing aggregates is illustrated in Fig. 3 together with the Trask parameters calculated from the quartiles of the graph. The calculated sorting coefficients attest to a well sorted stream sediment according to Pettijohn et al. (1973) and support the visual examination of a similar sediment from the northern study sites (Fig. 2d). The sphericity does not change very much as a function of grain size and comes close to an isometric shape (Fig. 3).

4.1.2. Sedimentary traps in plan view and cross section

The drainage systems in the NE Bavarian basement and its western foreland were hierarchically subdivided into three different classes according to their channel morphology, length and width. Further on, the higher orders were subdivided into subclasses based upon the prevailing type of country rocks along the thalweg and in the catchment area (Table 2). The descriptive classification scheme adopted for the drainage system in the current study follows largely the recommendations put forward by Miall (2006) on fluvial sedimentology. Numbering of the classes strictly follows the hierarchy in the drainage system, with

the large trunk river Donau/Danube given the class I, the tributary Naab River is denominated as class II and the smaller channels fall into class III. Unlike the rivers Donau and Naab, these small channels cannot be shown on the map in Fig. 1b but only in maps providing a geological close-up view of the study area, such as Fig. 4. This is due to the small size of the creeks whose width seldom exceeds more than one meter. Along with those parameters, defining a drainage system, the presence of "nigrine" and "antinigrine" is shown in another column together with some single HM grains of, e.g., columbite, which may be found in these titaniferous HM aggregates. By the end of the glacial period, channels of the present-day fluvial drainage systems incised into the rocks and shaped the northeastern part of the NE Bavarian basement which is characterized by a rather rugged terrain at an altitude of between 500 and 1000 m above mean sea level (a.m.s.l.) with rivers draining it mainly towards the S.

The area is covered by forests of coniferous trees, less frequently mixed up with softwood trees (Fig. 5a). Titaniferous HM aggregates are confined to the IIIa- and IIIb-class fluvial drainage systems, whereas its major components may be recognized all the way down to the class-I trunk rivers (Table 2). In plan view, these HM aggregates are restricted to the highest order within the fluvial hierarchy of the drainage systems, in cross section you may find them from the most recent channel system down to the bedrock–sediment interface preferably at the lowermost part in the channel lag deposits. In the present-day rivulet they are "baked" together at the lowermost part of the channels (Fig. 5b). In trenches cutting down into fining-upward class-III deposits titaniferous HM aggregates may be encountered in semi-consolidated channel lag deposits abundant in angular clasts underneath the grusy, arenaceous deposits (Fig. 5c).

4.2. Rutile–ilmenite aggregates—texture

Based upon detailed EMP and SEM-EDX analyses three major types of "nigrine" and "antinigrine" have been established for the study area (Table 1). These types, named A, B and C, contain rutile present as lamellae, forming the core zone of the aggregates and being concentrated along fissures intersecting ilmenite (Table 1). Rutile and ilmenite differ from each other with respect to their Nb, Fe, Cr and V contents. Some also have elevated W contents. "Antinigrine" with ilmenite exceeding the amount of rutile occurs among all three types of titaniferous aggregates (Table 1).

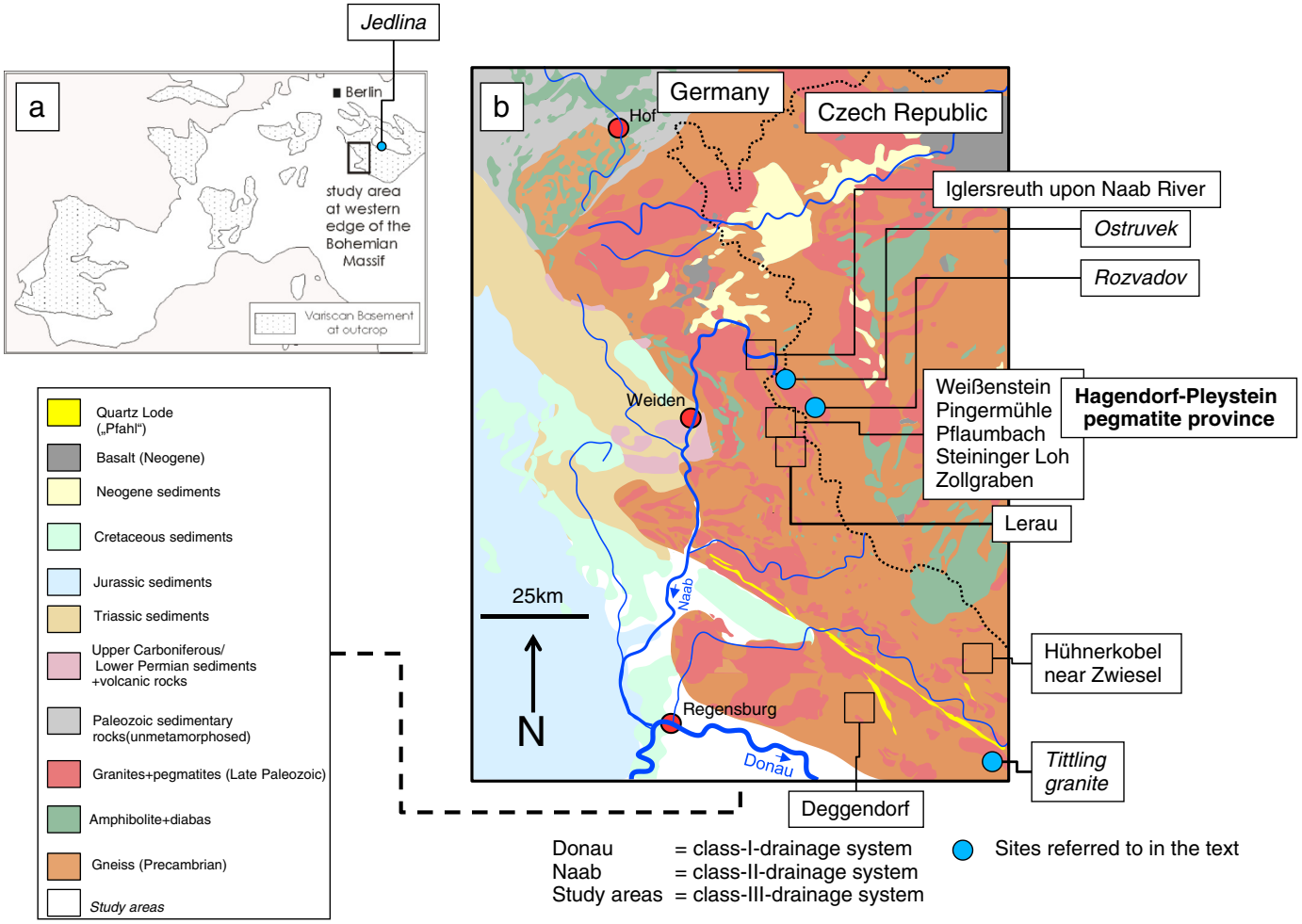

Fig 1. Sampling sites of "nigrine" and "antinigrine" and their geological setting within the NE Bavarian Basement, SE Germany.

a) Location of the study area relative to the European Variscides (Fig. 1b)
b) The NE Bavarian Basement, SE Germany, forming the western edge of the Bohemian Massif along the Czech–German border. The various sampling areas for "nigrine "and "antinigrine" referred to in the text are framed. Only the most prominent shear zones, e.g. "Pfahl" are shown in the geological map. Smaller ones which ran NW–SE or NNW–SSE cannot be visualized for reasons of scale. The hierarchical order of the drainage systems is shown in Fig. 1c (see also Table 2).
c) The three geodynamic units along the western edge of the Bohemia Massif, the Moldanubicum, the Bohemicum made up of the ZEV, the MM and the region of Teplá–Domažlice which covers part of the Moldanubicum and was also overriding the Saxothurigicum. The various sampling sites for "nigrine" and "antinigrine" are shown to follow deep-seated lineamentary fault zones and the contact between the allochthonous and autochthonous units. The viewer is looking at an exhumed thrust plane.

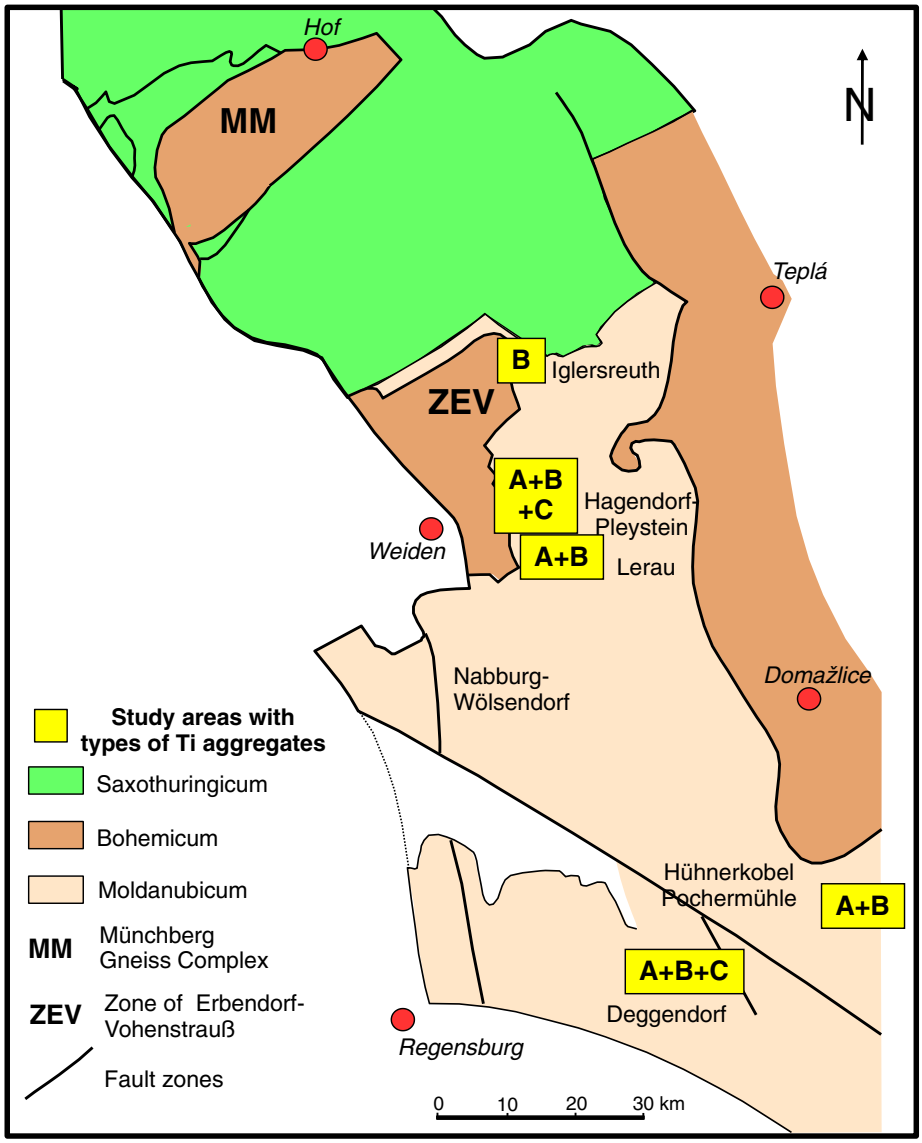

Fig. 1. (*continued*).

4.2.1. Type A

Excluding Iglersreuth, which is located in the northernmost part of the study area, type A "nigrine" was encountered in all sampling sites. The back-scattered electron image of Fig. 6a displays insular niobian rutile dispersed in ilmenite and replaced by pseudorutile. The latter mineral can be recognized as tiny irregular areas within ilmenite, being darker than the matrix ilmenite. The most common textural type is illustrated in Fig. 6b where rutile and ilmenite are regularly intergrown with each other. Apart from these common types, zoned grains with trellis-like ilmenite lamellae in "nigrine" are observed. In "antinigrine", massive grains of ilmenite have fissures filled with zoned rutile or rutile inclusions scattered throughout ilmenite. Inclusions of minerals other than titaniferous ones are seldom in type A.

4.2.2. Type B

From the textural point of view the intergrowth of rutile and ilmenite is more complex in type B and the structural features are finer than in type A. Mineral inclusions bearing elements other than Ti are more widespread and more variegated (Section 4.4). Fig. 6c displays slender lamellae of niobian rutile intergrown with ilmenite in "nigrine"-type B. Small irregularly-shaped grains of columbite-(Fe) are common in this type. Dendritic to graphic intergrowth of lath-shaped rutile is common in this type of "nigrine" (Fig. 6d). Ilmenite rims the "nigrine" aggregates and the titaniferous aggregates are replaced by pseudorutile and "leucoxene". Exsolution lamellae of low-trace-element rutile and niobian rutile are both found in the same mineral aggregates. The lamellae of rutile developed from the core into the rim. In "antinigrine", a lamellar intergrowth texture has not been observed, but rutile grains formed instead.

4.2.3. Type C

Type C is rather uncommon among the "nigrine"-types and characterized by lamellae of W-bearing rutile criss-crossing each other in rutile (Fig. 6e). In contrast to this special type C, W enrichment in type B "antinigrine" goes quite a different way with myriads of wolframite blebs scattered in the titaniferous phases (Fig. 6f).

4.3. Rutile–ilmenite aggregates—chemical composition

The most diagnostic elements Nb and Fe are listed in Table 1 for each type of "nigrine" and "antinigrine". Due to its massive texture and moderate changes in its chemical composition, ilmenite does not justify any further subdivision of its chemical composition as a function of texture (Table 1). Contrary to ilmenite, the various textures of rutile force to a

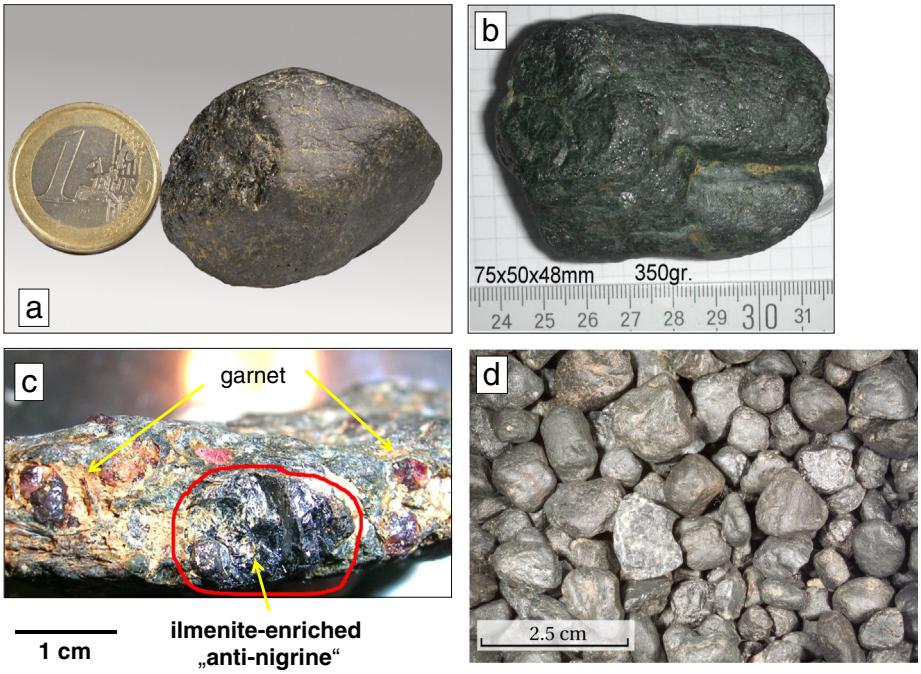

Fig. 2. Grain morphology of Ti-bearing heavy mineral aggregates.

a) "Antinigrine" from alluvial–fluvial deposits of the Goldbach in the Deggendorf study area
b) The largest "antinigrine" gravel from colluvial deposits near Aslach in the Deggendorf study area
c) "Antinigrine" within a garnet-bearing sillimanite gneiss near Aslach in the Deggendorf study area
d) Complex ilmenite–rutile intergrowth of "nigrine" type A 1 from the Pflaumbach fluvial deposits near Pleystein in the Hagendorf–Pleystein pegmatite province.

differential diagnosis of the three rutile subtypes, (1) rutile in the core zone,(2) lamellar and grainy rutile and (3) rutile in fissures. Rutile type A reveals lower niobium contents than type B for all its subtypes, excluding rutile when making up the core of "nigrine" type A. The most elevated Nb contents were met in rutile from the fissures intersecting type B "nigrine". The lowest Nb contents can be reported for type C where Nb_2O_5 values do not exceed 1.0 wt.% (Table 1). The Nb_2O_5 contents of rutile reach 31 wt.%, and thus are higher than values of up to 26.34 wt.% Nb_2O_5 which were reported by Černý et al. (2007) from granitic pegmatites of the Písek region, Czech Republic, located further to the East within the Bohemian Massif. What makes this Nb-bearing rutile in SE Germany so much different from rutile in the center of the Bohemian Massif is the variety of trace elements, e.g., Fe, Ta, W, Zr and Hf, compared to the Nb rutile found in "nigrine" from the western edge of the Bohemian Massif. Only W is slightly increased in type C rutile, yet at a low Nb level (Table 1). Numerous other diagnostic elements have been recorded from rutile of rather exotic depositional environments but have not been found in titaniferous aggregates in Germany so far (Graham and Morris, 1973; Smith and Perseil, 1997; Urban et al., 1992).

Niobium and tantalum are positively correlated with each other in all types under study (Fig. 7). Only type A from the Hühnerkobel and the Hagendorf–Pleystein regions are Ta-dominated. The remaining types are characterized by Nb contents exceeding the Ta contents of rutile.

Cobbles and pebbles of Ti aggregates were sampled from colluvial and alluvial through fluvial deposits spread across the crystalline basement rocks at Deggendorf (Fig. 5a) and analyzed for their Nb contents which were plotted in form a histogram relative to the geological setting (Fig. 4). The most elevated contents were reported from station point F1a, yielding 4238 ppm Nb. The lowest amount with 596 ppm Nb was found at sampling point F 3 within a swarm of quartz diorites (Fig. 4). The stream sediments of the study area near Deggendorf not only show abnormally high values for Nb, but also for REE and Ta (Table 3). For that reason, different drainage systems have been sampled at different distances from phosphate-bearing Nb–Ta pegmatites at the western edge of the Bohemian Massif to see whether these elements vary relative to the distance from pegmatite. Panned stream sediments, enriched in "nigrine" and/or "antinigrine" were subjected to whole rock chemical analysis and the resultant chemical data subjected to an inter-element correlation. In Table 4 the correlation coefficients of the more than 100 samples between Ti and several elements abnormally enriched in the area have been plotted as a function of distance from pegmatites for various environments of deposition. The majority of samples show ambivalent characters with positive and negative coefficients of correlations, e.g. Nd and Rb. Some elements like phosphorus and yttrium show an overall negative correlation with titanium in all depositional environments, but do not disclose any trend (Table 4). Cesium, tin and tantalum reveal a positive correlation with titanium, but similar to phosphorus and yttrium do not show a trend. The highest correlation coefficient with $r = +0.92$ was achieved for niobium in the Pflaumbach drainage system which cuts into the roof rocks of a pegmatite and whose silica core is exposed approximately 1 km away from the sampling site. Niobium is the only element which reveals a clearcut trend of its correlation coefficient, gradually diminishing from +0.92 through +0.42 away from the pegmatite (Table 4).

4.4. Minerals associated with "nigrine" and "antinigrine"

4.4.1. Columbite and pyrochlore-type minerals

Columbite is the most common constituent among the accessory minerals of type B "nigrine" and also of widespread occurrence in pegmatites elsewhere in the Bohemian Massif (Table 1, Figs. 6c, 8a) (Novák and Černý, 2001). It is exclusive to this type of titaniferous aggregates. Nigrine-hosted columbite from the stream sediments can be denominated as columbite-(Fe) (Table 5). In the entire study area there are mainly columbite group minerals with Nb exceeding the content of Ta and with Fe prevailing over Mn (Klinger and Sperling, 2008). This is also true for the columbite group minerals encountered in the pegmatites of Hagendorf, Pleystein, Hühnerkobel and the Trutzhofmühle

Table 1
Tripartite subdivision of "nigrine" (red) and "antinigrine" (blue) in the NE Bavarian Basement according to their texture, chemical composition, mineral assemblage and sampling locations. The column "Inclusions" reports on minerals of the primary environment of formation and may also be used as tool for exploration, while the column "Alteration" provides the secondary minerals filling vugs and cavities of the HM aggregates and indicative of the chemical weathering and the regime on transport.

Sampling location	Type	Range	Size	Rutile core		Rutile lamellae/grains		Rutile in fissures		Ilmenite		Inclusions					I+A	Alteration		
		mm		Nb_2O_5	FeO	Nb_2O_5	FeO	Nb	FeO	MnO	Nb_2O_5	Columbite	Pyrochlore	Monazite–xenotime	Zircon	Minor constituents	Hematite–magnetite	Pseudorutile	Ti–Al–P–Fe ox	Nb–Ti–Ta–P
Weißenstein Pflaumbach Steininger Loh Pingermühle Deggendorf Zwiesel	A	min	0.4	0.3	0.2	1.1	0.5	0.0	0.0	0.8	0.0			x		sph, po		x	x	
		max	11.0	6.6	6.6	10.0	4.8	12.6	1.0	4.0	0.5									
Pingermühle Iglersreuth Tirschenreuther Zwiesel Deggendorf	B	min	3.0	0.3	0.4	0.0	0.1	0.3	0.0	1.14	0.0	x	x		x	U–pyr.	x	x	x	x
		max	6.0	0.4	0.8	26.6	15.0	30.9	0.9	9.0	1.2									
Pflaumbach Deggendorf	C	min	0.5	0.2	0.5	0.2	0.0			2.1	0.0									
		max	8.0			0.3	2.0			2.2	2.0									

Sph = sphalerite, po = pyrrhotite, U-pyr = uraniferous pyrochlore, Ti–Al–P–Fe ox = "leucoxene" + "limonite" + aluminum phosphates, I + A = inclusion plus alteration.

aplite near Pleystein, which are plotted together with their correlative stream sediment-hosted columbite in Fig. 9.

There is a tendency of columbite-(Fe) in titaniferous aggregates from stream sediments (Deggendorf, Iglersreuth, Pflaumbach) to be lower in Ta than the correlative pegmatite-hosted (Hagendorf, Pleystein, Hühnerkobel-Pochermühle) and aplite-hosted columbite group minerals (Trutzhofmühle). Two different trends are to be recognized and represented by their skewness values or in graphic terms, by the inclination of the trend lines in Fig. 9. In the northern part of the study area, a positive trend exists from stream sediments (Pflaumbach (0.205x), Iglersreuth (0.4649x)), to pegmatite-hosted columbite Hagendorf (5.6478x), and Pleystein (7.1968x); this is a classical trend during fractionation of pegmatitic melts. In the southern region a negative trend gives way from stream sediments (Deggendorf 2 (−0.1028x)), via Hühnerkobel–Pochermühle (−3.4677x) through Deggendorf 1 (−4.9165x), both of which are representative of true pegmatite-hosted Fe-enriched columbite group minerals (Figs. 1, 9). Titaniferous stream sediments in the clastic apron around the pegmatites and aplites well fit into the trend observed within the pegmatites and aplites proper (Fig. 9). For discussion see Section 5 (Linnen and Keppler, 1997). Aplite-hosted columbite of Trutzhofmühle (1.5497x) which also differs in shape from the overall pegmatites goes a different way.

High concentrations of Ti, Sc and W seem to be typical of the province (Dill et al., 2008b).

Columbite-(Fe) is replaced by pyrochlore in type B "nigrine". According to the relations Nb + Ta > 2Ti and Nb > Ta the detected mineral inclusions qualify for a member of the pyrochlore group (Hogarth, 1977). Only recently the pyrochlore group minerals were undergoing a reclassification leading to its promotion as a supergroup of minerals and a new denomination (Atencio et al., 2010). The calculated average formula of $Ca(Nb_{1.78}Ta_{0.04}Ti_{0.16}Fe^{3+}{}_{0.06})_2O_6$ points to an aeschynite-type mineral $[(Ce,Ca,Fe,Th)(Ti,Nb)_2(O,OH)_6]$ that can be described as niobioaeschynite. Aeschynite is accompanied by betafite $[(Ca,U,\square)_2(Ti,Nb,Ta)_2(O,OH)_7]$ sensu Nickel and Nichols (2004) which in some grains measuring up to 30 μm in size contains U of as much as 29 wt.% UO_2, yielding an average formula of $(Ca_{1.1}Na_{0.2}U_{0.4})_{\Sigma 1.7}(Nb_{1.0}Ta_{0.1}Ti_{0.9})_{\Sigma 2.0}(O,OH)_7$.

According to the newly introduced classification scheme of the pyrochlore supergroup by Atencio et al. (2010) the latter minerals is a solid solution series of oxyuranobetafite and oxynatropyrochlore.

4.4.2. Wolframite

Unlike columbite group minerals and pyrochlore group minerals, wolframite is known from type B- and rarely from type A "nigrine" too (Fig. 8b). Some "nigrine" samples are peppered with myriads of tiny grains of wolframite (Fig. 8b). According to the chemical data listed in Table 5, the chemical composition of wolframite varies only in a very narrow range and may be denominated as a ferberite.

4.4.3. Titanium–niobium–aluminum–iron-phosphate minerals

There are chemical compounds with Ti exceeding the amount of phosphate by some orders of magnitude. One chemical compound is dominated by niobium. The chemical composition points to a Ti–Al–Fe–P phase for which we could not find any corresponding chemical composition in the common tables for mineralogy, so that in this paper it is still treated as an unknown mineral or a nano-scale intergrowth of an Al–Fe phosphate with some kind of "leucoxene". Others may simply be a mixture of different chemical compositions caused by the intimate intergrowth of minerals of very small grain size and as such they are not listed in Table 5. The true nature cannot be disclosed by means of the methods applied during this study.

4.4.4. Titanium–iron and iron compounds

Rutile and ilmenite constitute the major components of "nigrine" and "antinigrine". Besides these major Ti minerals another Fe–Ti mineral occurs which has been given different names such as "hydroilmenite" (Frost et al., 1983) and "leached ilmenite" (Mücke and Bhadra Chaudhuri, 1991). The official term accepted by IMA is pseudorutile (Grey et al., 1994) having Ti/(Ti + Fe) ratios between 0.6 and 0.7 (Table 5). The textural relation between rutile, ilmenite and pseudorutile which developed in type A- and type B-titanium aggregates is made visible in the BSE image of Fig. 6a and d.

Hematite and magnetite were only found filling fissures or being included in ilmenite or rutile (Table 5). Magnetite is almost barren as to

trace elements except titanium that attains a value of 3.22 wt.% TiO_2. Iron oxides only show up in the type B Ti aggregates.

4.4.5. Zircon, spinel, xenotime and monazite

The REE phosphates monazite and xenotime as well as zircon are sporadically included in "nigrine" and "antinigrine" (Table 5, Fig. 8c, d, e, and f). In places, one may observe these mineral grains also as single grains, removed from their HM aggregates by attrition upon transport (Fig. 8d). The latter mineral grains in the stream sediments are fragmented and no longer found with their crystal shape well preserved. Zircon is common to type B, whereas monazite and xenotime are included in type A Ti-bearing mineral aggregates (Table 5, Fig. 8c, d, e, and f). Despite being among the rare constituents, their outward appearance shows a rather variable morphology and reveals complex crystal shapes which are described using the Miller's indices for labeling of the individual faces. A characteristic feature of zircon in "nigrine" are the prismatic faces (110), the pyramid faces (211) and (110) (Fig. 8c). Monazite crystals are found next to octahedral hercynite in gneissic wall rocks of "nigrine". Monazite demonstrates as a typical feature the faces (101), while spinel has a rather complex morphology. The common (111) faces are supplemented by subfaces (110) and (211) (Fig. 8e, f).

4.5. Chemical composition of siliceous shear zones

The quartz mineralization along shear zones at the western edge of the Bohemian Massif was investigated for their chemical composition and its trace elements were listed in Table 6. The detailed chemical analysis was performed to get an insight into the temperature of formation along the shear zones that also gave host to the titaniferous mineral aggregates. The Ti-in-quartz geothermometer of Wark and Watson (2006) provides a tool to determine the quartz crystallization temperature based on the temperature dependence of the Ti^{4+}–Si^{4+} substitution in quartz and given the presence of rutile or, in its absence, an estimate of the TiO_2 activity of the system.

This geothermometer can be applied for temperatures up to as much as 1000 °C.

According to both authors, the Ti contents of quartz given in ppm by weight increase exponentially with reciprocal T as described by the equation:

$$\mathrm{Log}\ X^{qtz}_{Ti} = (5.69 \pm 0.02) - ((3765 \pm 24)/T(K))$$

Quartz from these shear zones under study crystallized in the range 730.9 °C down to 470.2 °C (Table 6).

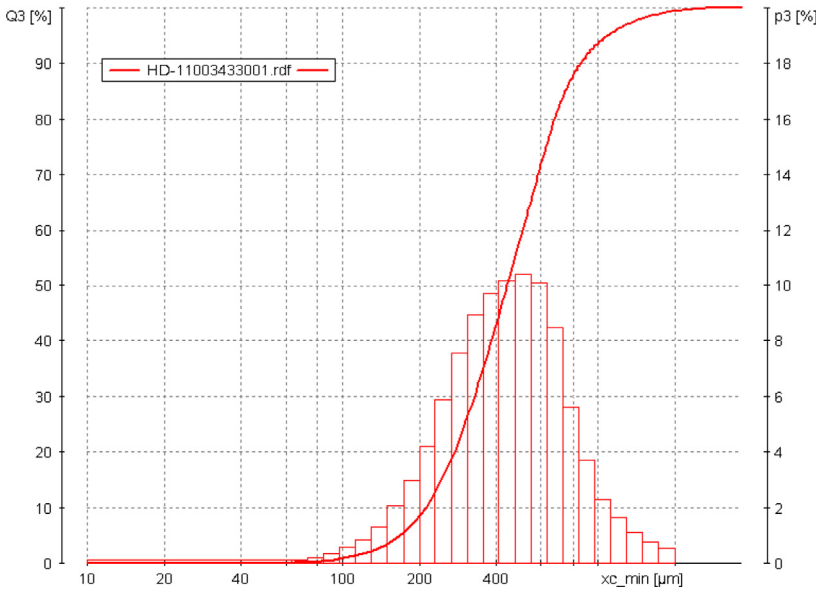

Median	Sorting		Skewness	
MD (in µm)	SO	so	SK	LOG(SK)
440	1.445	2.087	0.969	-0.0135

Median =MD = quartile Q 2
Sorting SO = (Q3/Q1)½
so = Q3/Q1
Skewness = (Q1*Q3)/MD²

grain size class	0	84	112	173	200	266	409	472	630	728	1120	1494	1725	2000
[µm]	63	97	129	200	230	307	472	546	728	840	1294	1725	2000	>2000
sphericity	0.847	0.879	0.879	0.861	0.865	0.858	0.85	0.845	0.885	0.878	0.863	0.853	0.834	0.818

Fig. 3. Grain size variation of a typical arenaceous stream sediment from a fluvial drainage system in the Deggendorf area dominated by titaniferous heavy mineral aggregates. The grain size is expressed as a histogram and as a cumulative frequency grain size distribution curve. The Trask parameters are given below as it is the case with the equations leading to the median, sorting coefficients and skewness. The morphological parameters can be deduced from the sphericity and the ratio length:width.

Table 2
Depositional environments in the NE Bavarian Basement and its foreland containing "nigrine" and "antinigrine" as well as single grains of those HM used to be found included in these titaniferous HM aggregates as armored relics. The numbering of the drainages system starts off from the largest trunk river in the region, the Donau River, given the number I and ends up in the basement area with class-III drainage channels.

Placer-type	Drainage type		Occurrence of "nigrine" and "anti-nigrine" and associated minerals in the placer deposits	Mechanical stability (for distance see Fig. 1b)
	Host and source rock in the catchment area	Class		
Colluvial-alluvial,-(fluvial) placers	Straight creeks with a small catchment area Gneiss, diorites	IIIb	Magnetite, rutile, "nigrine", "anti-nigrine", ilmenite	Stability fields of "nigrine-anti-nigrine"
Alluvial-fluvial placer	Branched drainage system of small rivulets Gneiss, aplite, pegmatite, quartz veins, amphibolite	IIIa	Rutile, rutile-(Nb), ilmenite, "nigrine", columbite	onset of release of columbite from HM aggregates
Alluvial-fluvial placers	Branched drainage system small rivulets Upper Cretaceous siliciclastics, Permo-Carboniferous sediments and volcaniclastics, amphibolites	IIIa	Magnetite, ilmenite (pyrophanite), rutile, anatase, hematite	Stability field of columbite (only in the upper reaches, near the confluence of class II with class IIIa channels
Alluvial-(fluvial) placer	Branched drainage system small rivulets Gneiss, granite, quartz veins	IIIa	Ilmenite, rutile, "leucoxene"	and "leucoxene" and anatase
Fluvial placer Naab-River drainage system	Tributary river system Basement and Mesozoic through Cenozoic foreland sediments	II	Magnetite, hematite, xenotime, columbite, rutile, ilmenite	
Fluvial placer (trunk river) Donau-River drainage system	Trunk river system Basement and Mesozoic through Cenozoic foreland sediments	I	Ilmenite, hematite, rutile, magnetite	Stability field of iron- and titanium oxides only

5. Discussion

5.1. Textural relationship between titaniferous HM aggregates and their country rocks

A-type "nigrine" has been encountered in hard rocks, mainly in gneisses, in silicification zones, and in quartz dykes (Fig. 10a). In one of the insular- or core-type A-type "nigrine" samples, a sequence of mechanical and chemical processes was observed that allows a precise timing of the "nigrinisation" relative to the deformation affecting the country rocks of these Ti compounds (Fig. 10a type A). The process started off with undistorted exsolution of ilmenite from Nb rutile, followed by kinking of exsolution lamellae of ilmenite in niobian rutile and eventually ended up with normal faulting of ilmenite, whereby exsolution lamellae of ilmenite are thrown against Nb rutile (Fig. 10a). Asymmetric kink bands, such as illustrated in Fig. 10 for the first time in an isotropic "nigrine" aggregate, are commonly described from low-grade regionally metamorphosed ductile phyllites, mica schists and strain-related shear zones. The quartz-bearing fault system hosting "nigrine" in the NE Bavarian Basement forms part of the strain–stress system of the "Pfahl" zone (Fig. 1). The northwest-striking "Pfahl" zone is a mylonitic shear zone that is associated with brittle–ductile deformation fabrics and a conspicuous hydrothermal quartz mineralization. It has also some en echelon faults running N–S to the main NW–SE quartz dyke. Two granites from this shear zone yield U–Pb and Pb–Pb evaporation ages between 321 and 329 Ma and two granodiorites give concordant ^{238}U–^{206}Pb and ^{235}U–^{207}Pb ages of 325 ± 3 Ma and 326 ± 3 Ma, respectively (Siebel et al., 2006). One granite body is transected by the shear zone but the main mass of the granite is largely undeformed. This finding suggests that granite intrusion predates the final stage of ductile deformation along the Pfahl shear zone (Siebel et al., 2006). The maximum quartz temperature of which is close to 730 °C. Type A "nigrine" is pre- to synkinematic relative to the shearing in the quartz-bearing fault system. Its samples are also ubiquitous in the stream sediments. The temperature of formation coincides with the data array obtained for the temperature of formation of the quartz dykes at Rozvadov and Ostruvek, being located immediately east of the Czech–German border (Fig. 1, Table 6).

Type B "nigrine" is widespread in stream sediments of pegmatite–aplite provinces but has not been found in host rocks such as pegmatites. The grains of type B nigrine do not show any deformation and, hence, have to be described as postkinematic relative to the last tectonic activities of the Variscan orogeny (Fig. 10b). It is assumed to have formed in the topmost parts or roof rocks of the pegmatites. At 311.9 ± 2.7 Ma the postkinematic Flossenbürg Granite was intruded into the crystalline basement; the columbite-(Fe) of the Trutzhofmühle aplite was dated at 302 ± 3 Ma (Dill et al., 2008b; Wendt et al., 1994). Both ages reflect the period of time during which granites and pegmatites were emplaced at the western edge of the Bohemian Massif but postdate the pegmatites in the central parts of the Bohemian Massif, where columbite yielded an age of formation between 333 ± 3 Ma and 325 ± 4 Ma, signaling a different level and period of emplacement (Melleton et al., 2012).

Type C "nigrine" (W-bearing "nigrine") was found in the quartz dykes as well as in the streams sediments, yet only to a minor extent

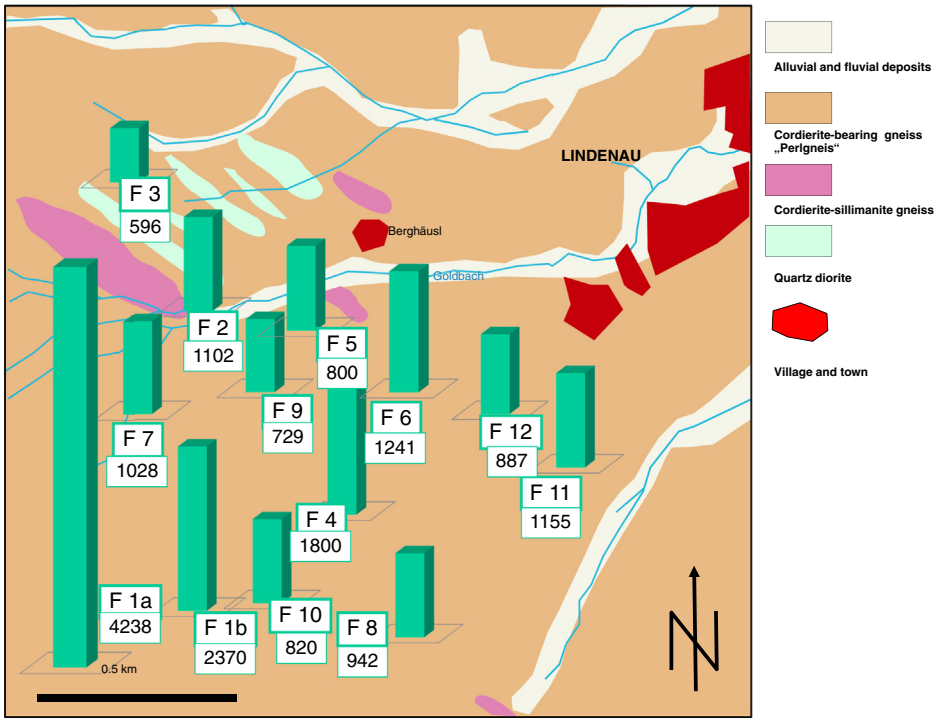

Fig. 4. The study site near Deggendorf shows the regional geology, the class-III drainage system and the niobium contents in titaniferous HM aggregates at various sampling sites around the Goldbach Creek. The niobium contents were plotted in form a columns relative to the geological setting to illustrate the abnormally high values and demonstrate the genetic link between the regional geology and the geomorphology (drainage system). The numerical values are given in ppm.

(Fig. 10c). It is undeformed like type B and postkinematic as to the structural disturbances of its host rocks. It reflects the youngest structural processes along the quartz mineralization during the late Variscan tectonic deformation in the NE Bavarian Basement. Its temperature of formation is as low as 470 °C (Fig. 10c). Fig. 10d shows a younger stage than in Fig. 10c but the stage reflects already the destruction of the primary mineralization during supergene alteration.

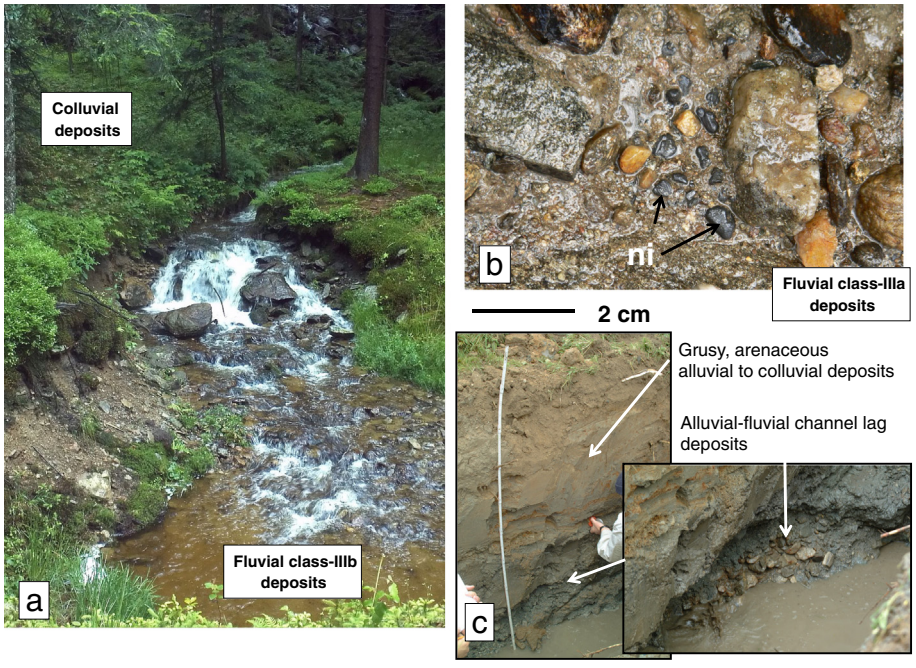

Fig. 5. The sedimentary traps of “nigrine” and “antinigrine” within the tripartite hierarchical subdivision of alluvial–fluvial deposits in the NE Bavarian basement and its foreland.

a) A typical class-IIIb drainage system containing titaniferous HM aggregates along the thalweg and along its flanks within the colluvial deposits in the Goldbach drainage system near Deggendorf. See also Fig. 4 for geology
b) Present-day “blue-ground-like” deposits of “nigrine” (ni) in oligomictic gravel bed of a class-IIIa drainage system near Pleystein
c) Late Pleistocene fining-upward sediments with “nigrine” in channel lag deposits at the bedrock–sediment interface of a class-IIIa drainage system near Pleystein. Yardstick is 2 m.

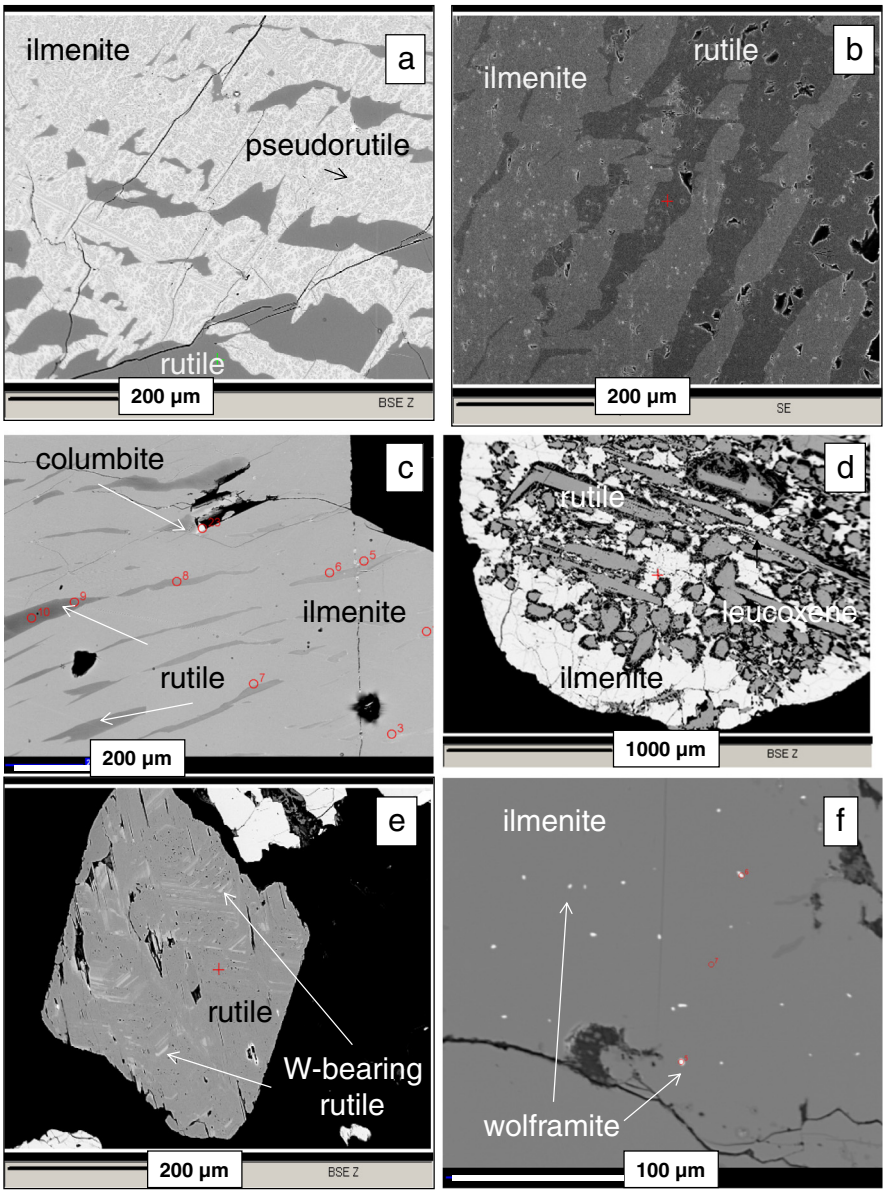

Fig. 6. Micrographs of "nigrine" and "antinigrine" (BSE imagery).

a) "Nigrine" type A showing insular niobian rutile rimmed by ilmenite and replaced by pseudorutile (white tiny lamellae within ilmenite) (Zwiesel)
b) "Nigrine" type A lamellar intergrowth of rutile and ilmenite (Zwiesel)
c) "Nigrine" type B slender lamellae of niobian rutile intergrown with ilmenite. Small irregularly-shaped grains of columbite-Fe are visible (Zwiesel)
d) Dentritic to graphic intergrowth of lath-shaped rutile in nigrine of type B. Ilmenite rims the "nigrine" aggregates. The "nigrine" aggregates are replaced by pseudorutile and "leucoxene" (Pleystein Pflaumbach)
e) Nigrine type C. Rutile with exsolution lamellae of W-enriched rutile (Pleystein Pflaumbach)
f) "Antinigrine" type B made up of ilmenite peppered with wolframite (Deggendorf).

5.2. Classification of minerals within the titaniferous mineral aggregates

Major and minor minerals in "nigrine" and "antinigrine" HM aggregates fall into two classes. The primary minerals rutile and ilmenite including some minor constituents shed some light on the origin of these Ti aggregates. They are the most decisive minerals and may act as an ore guide during exploration, enabling us to describe the source area (Table 1).

Primary Fe–Ti minerals were corroded and altered to secondary minerals at their edges or along fissures, such as anatase (only found as isolated grains in the stream sediments or intimately intergrown with other oxidic compounds in "leucoxene" and pseudorutile). They form part of the secondary minerals or alteration minerals together with complex Ti–Al–P–Fe oxides and Nb–Ti–Ta–phosphate-oxide compounds (Table 1).

The iron oxides, magnetite and hematite were not assigned to any specific group as they form the missing link between the two groups with magnetite being part of the primary minerals and hematite bridging the gap into supergene alteration.

5.3. Primary minerals and the physical–chemical regime of the source rocks

5.3.1. Ilmenite

Ilmenite associated with rutile in "nigrine" and "antinigrine" has rather low Nb_2O_5 contents when compared to those of rutile (Table 1). This is also the case with MgO, whereas MnO can achieve contents of as much as 9.4 wt.% MnO in ilmenite, particularly in type B "nigrine". While the geikielite [$MgTiO_3$] component does not play a genetic role in the ilmenite group minerals under study, pyrophanite [$MnTiO_3$] does so (Feenstra

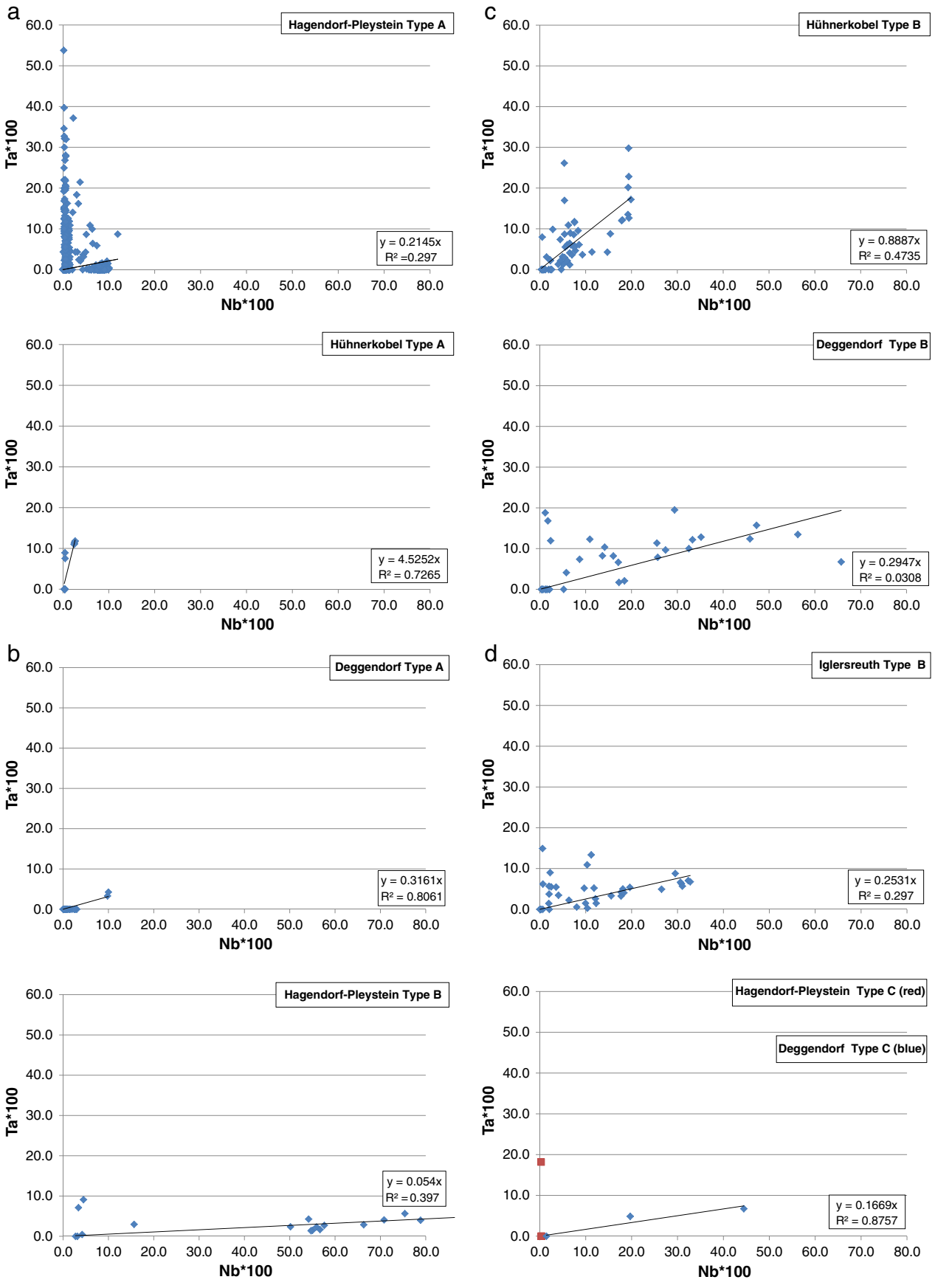
a
Hagendorf-Pleystein Type A
y = 0.2145x
R² =0.297
c
Hühnerkobel Type B
y = 0.8887x
R² = 0.4735
Hühnerkobel Type A
y = 4.5252x
R² = 0.7265
Deggendorf Type B
y = 0.2947x
R² = 0.0308
b
Deggendorf Type A
y = 0.3161x
R² = 0.8061
d
Iglersreuth Type B
y = 0.2531x
R² = 0.297
Hagendorf-Pleystein Type B
y = 0.054x
R² = 0.397
Hagendorf-Pleystein Type C (red)
Deggendorf Type C (blue)
y = 0.1669x
R² = 0.8757
Ta*100
Nb*100

and Peters, 1996). Sakoma and Martin (2002) presumed a moderately increased MnO content in ilmenite from the Tibchi ring complex, Nigeria, to have resulted from fractionation in the melt, while a stronger enrichment of the pyrophanite component in ilmenite is explained by hydrothermal processes which introduced Mn into the system under study. Our data speak in favor of a differentiation process rather any hydrothermally induced Mn contents in ilmenite. Apart from that, the overall presence of ilmenite relative to pseudorutile and the absence of TiO_2 components such as anatase or brookite stress an Eh < 0 in the source rock (Warenborgh et al., 2002).

5.3.2. Rutile

Excluding type C "nigrine", the Nb contents in cored and lamellar rutile from titaniferous HM aggregates are abnormally high, thus qualifying it as niobian rutile ("ilmenorutile") which is not unusual in pegmatitic systems (Černý et al., 1999, 2000, 2007). Low Nb concentrations in rutile are explained by a low capacity of fluids for transporting high field strength elements (Xiong et al., 2005). Rutile from mafic rocks have up to 1500 ppm Nb, increasing to 3000 ppm (rarely 28,000 Nb) in metapelitic rocks (Zack et al., 2004). Niobium and tantalum can substitute for titanium according to the equation $5Ti^{4+} \Rightarrow 4\ (Nb,Ta)^{5+} + \square$, where one vacancy has to be claimed to attain electrostatic charge balance. The most likely source for titanium in our HM aggregates is Ti-bearing biotite or Ti-bearing hornblende being subjected to mineral conversion during retrograde processes and undergoing chloritization (Müller, 1966). Low Nb rutile is interpreted to have derived from Ti-bearing mafic minerals during retrograde metamorphism. Niobian rutile, however, is held representative of the pegmatitic mobilization in the course of shear processes along the deep-seated lineaments such as the "Pfahl". Friction at depth provided the heat to mobilize alkaline solutions and fracture propagation fostered their ascent into shallower parts of the crust, where the cooling mass can take a more tabular shape at the beginning fractionation or get emplaced as a stock at a more advanced level of differentiation-see also (Clemens, 1998) (Figs. 1, 10). Titanium is not directly involved in this process of mobilization, otherwise its minerals should show up in the resultant intrusive igneous rocks. The Ti minerals acted as some kind of a proximity indicator in the crystalline country and wall rocks surrounding the pegmatites, instead. The Nb-bearing type B "nigrine" grew proximal to the pegmatite, whereas type A takes a more distal position relative to the pegmatite. It is a marker for the shear zone at its best. With this in mind the different contents of Nb from the Deggendorf test region, which is located immediately south of the "Pfahl" near one of its "en echelon" parasite faults, are likely to have been caused by a Nb source in form of a pegmatite underneath the gneissic roof rocks (Figs. 1, 4, and 7). The primary source of Ti-in-nigrine has to be looked for within the metapelitic country rocks of the shear zones whose maximum Nb contents come close to the lower level of rutile in the "nigrine" aggregates (Table 1).

5.3.3. Columbite and pyrochlore

Columbite-(Fe) may be encountered in the pegmatites and in the stream sediments, either incorporated into Ti-bearing HM aggregates or set free from them as individual HM grains in the lower reaches of class III and upper reaches of class-II drainage systems (Fig. 9). The samples of columbite-(Fe) significantly differ from each other by their Nb/Ta ratios. According to Aleksandrov (1963) and Linnen and Keppler (1997) the Ta/Nb ratio increases during fractionation. This is the most decisive act which brings together columbite-(Fe) from the sediments and the pegmatites and which has implications for the evolution of pegmatites and for the exploration on pegmatites containing Nb–Ta minerals. Type A (Fig. 10a) and type C (Fig. 10c) nigrine/antinigrine will not be considered here, because they are devoid of Nb–Ta minerals and therefore have little meaning as proximity indicators in the immediate surroundings of the pegmatites, where type B are the most crucial representatives of this type of mineral intergrowth (Fig. 10b). This trend refers to Nb–Ta-bearing phosphate pegmatites and aplites as they were described from a great many localities across the world, among others from the Bohemian Massif (Novák and Černý, 1998).

Mobilization of pegmatitic melts and their emplacement in form of tabular (e.g. Trutzhofmühle) and stocklike pegmatitic bodies (e.g. Hagendorf) was preceded by the growth of columbite-bearing nigrine/antinigrine in the roof rocks of the pegmatites and aplites, forming a sort of a halo around these felsic melts in their statu nascendi. These gneissic wall rocks contain the least fractionated mineral grains of columbite-(Fe), such as at Deggendorf 2, Plaumbach, Iglersreuth and hold the lowest Ta contents. As these gneissic rocks are located closer to the surface they got eroded first, much earlier than the pegmatitic mobilizates underneath, resultant in stream sediments containing Ta-poor columbite-(Fe).

Second in the succession of mobilization and emplacement of these felsic melts, tabular aplites of the Trutzhofmühle-type and Degendorf-2 type formed with an intermediate Ta/Nb ratio. Their grains of columbite-(Fe) are still disseminated in the felsic mobilizates. Due to the small thickness of these aplite swarms and the disseminated mineralization they do not contribute to the built-up of equivalent nigrine/antinigrine aggregates in the surrounding stream sediments.

This true also for the most strongly fractionated pegmatites. The most elevated Ta contents are encountered within the stocklike pegmatitic intrusive bodies of Hagendorf, Pleystein and Hühnerkobel–Pochermühle, where the zone enriched in columbite-(Fe) is still unaffected by any erosion and was only opened up by the miners.

The fractionation is also well-expressed by the trend lines in the various successions, starting off with a rather flat line and fading out with a trend line of a pronounced skewness. It is a fractionation, whose initial part can no longer be encountered in its original host rock but only observed in the stream sediments as HM aggregates. Sedimentologists, geomorphologist and petrographers must cooperate to draw a full picture of lithogenesis of pegmatites.

Betafite and pyrochlore replacing columbite-(Fe) in type B-"nigrine" are related to the waning stages of the Hercynian heat event, by analogy with the findings of Drew et al (1990) in Bayan Obo, China, and thus may indicate a more advanced level of fractionation. Columbite in form of exsolution-lamellae in "nigrine" or along fissures intersecting "antinigrine" are both an integral member of the story of fractionation, even if the majority of the Ti-bearing aggregates is nowadays observed as re-deposited HM aggregates in the drainage systems due to their marginal position relative to the dynamo-metamorphic center of mobilization.

Columbite-(Fe) found as inclusions in "nigrine" and – rarely – free grains in the stream sediments must have been derived from fractionated late-stage granitic, aplitic or pegmatitic source rocks, as revealed by the tripartite subdivision of columbite-(Fe) in the previous paragraphs. There is no indication in the study area, that columbite-(Fe) grew under hydrothermal conditions. The few columbite analyses that are available from the aplites and pegmatites in the area (Hagendorf, Pleystein, Trutzhofmühle) point to rare-element pegmatites of the LCT family (Li, Cs, and Ta), in particular to the beryl-type of Černý (1989) and Černý (2005). Columbites-(Fe) in the study area are characterized by

Fig. 7. Niobian and tantalum contents in rutile types from the western edge of the Bohemian Massif. The trend lines and their mathematical parameters are given for all textural types, excluding type C from Hagendorf–Pleystein where only two samples could be provided.

a) Hagendorf–Pleystein and Hühnerkobel type A.
b) Deggendorf type A and Hagendorf–Pleystein type B.
c) Hühnerkobel type B and Deggendorf type B.
d) Iglersreuth type B, Hagendorf–Pleystein-type C and Deggendorf type C.

Table 3
Chemical composition of stream sediments in the Deggendorf area.

		Min	Mean	Max
SiO_2	wt.%	0.44	28.32	71.66
TiO_2	wt.%	0.34	29.51	49.65
Al_2O_3	wt.%	0.24	6.41	14.66
Fe_2O_3	wt.%	2.66	32.19	51.13
MnO	wt.%	0.04	1.26	2.40
MgO	wt.%	0.28	0.61	0.83
CaO	wt.%	0.01	0.67	1.62
Na_2O	wt.%	0.01	1.19	3.56
K_2O	wt.%	0.01	1.10	3.13
P_2O_5	wt.%	0.03	0.12	0.24
Ba	ppm	96	432	1100
Ce	ppm	36	369	1010
Co	ppm	5	32	62
Cr	ppm	25	266	672
Cs	ppm	23	30	40
Cu	ppm	18	36	49
La	ppm	29	191	483
Mo	ppm	3	4	5
Nb	ppm	13	1599	4238
Nd	ppm	13	164	459
Ni	ppm	6	13	20
Pb	ppm	5	18	42
Rb	ppm	14	35	74
Sb	ppm	31	38	51
Sc	ppm	17	69	117
Sm	ppm	14	44	87
Sn	ppm	13	15	20
Sr	ppm	3	69	189
Ta	ppm	4	208	567
Th	ppm	15	91	219
U	ppm	3	18	42
V	ppm	11	488	1420
W	ppm	4	77	127
Y	ppm	9	257	743
Zn	ppm	37	142	208
Zr	ppm	113	354	814

very low Mn enrichment, probably due to low F activities, and to an overall low to moderate Nb-Ta fractionation A few columbite-(Fe) crystals investigated by EMPA and LA-ICP-MS from various pegmatites in the Hagendorf province reveal extreme concentrations of Zr (median 9000 ppm), Hf (927 ppm) and U (2463 ppm), and low Mg, Sb, Bi, Y and REE. The pegmatite province is furthermore characterized by its abundance of phosphates, a Sc signature (kolbeckite, unnamed Sc-rich phosphates, see Dill et al., 2008), and the presence of U-rich phases (uraninite, liandradite–petscheckite) (Dill et al., 2007a, 2008b, 2008c; Mücke and Keck, 2008).

Nb- and/or Ta-rich rutile is not a common mineral in rare-element pegmatites themselves, because Ti concentrations in pegmatite melts are usually low, and the available Ti is incorporated either into biotite, or into early columbite and tapiolite-see previous sections. However, there are some provinces where Nb–Ta-rutile is common and even economic. These include the placers found on the Archaean Man Shield (ilmenorutile with Nb > Ta; Sierra Leone) and the Mesozoic Jos Plateau, Nigeria (ilmenorutile, derived from anorogenic rare-metal biotite granites press), as well as the rare-element granites of Orlovka (Russia) (Melcher et al., 2008). Strüverite (Ta > Nb) is locally common in alluvial mineralizations in Central Africa (DR Congo, Rwanda), and in Panafrican LCT-pegmatite of Marropino (Mozambique), whereas both ilmenorutile and strüverite occur in fluvial placers of eastern Colombia, associated with columbite-(Fe), cassiterite and wolframite.

5.3.4. Wolframite

Wolframite from whatever type of HM aggregate it may be is enriched in Fe with FeO contents in these "nigrines" much higher than in granitic Sn–W-quartz veins, which fall in the range 16 to 17 wt.% FeO (Antunes et al., 2002) (Table 5). The wolframite and late W-bearing "nigrine" has all hallmarks of a hydrothermal/supercritical mineralization. Based upon the titanium-in-quartz geothermometer of Wark and Watson (2006) the W-bearing minerals within these titaniferous aggregates precipitated in the T range between 400 °C and 500 °C at rather shallow depth (Fig. 10c). Similar temperatures were also determined for the Jedlina "Pfahl" being exposed more central in the Bohemian Massif.

5.3.5. Monazite, xenotime and zircon

Monazite, zircon and xenotime do not contribute much to the REE budget and as such are irrelevant for any prediction about the economic geology of REE in this area and the pegmatites, in particular. Their strong points lie within the field of constraining the physical–chemical regime of formation and as a tool to for the source analysis based on crystal morphology. The crystal morphology of zircon shows an extreme variability and consequently has encouraged mineralogists to correlate the crystal habit with the environment of formation (Benisek and Finger, 1993; Bingen et al., 2001; Pupin, 1980). Type L 2 according to Pupin (1980) is the only type of zircon correlative with type A and B nigrinisation in the southern area, in the northern area no correlation between zircon and "nigrine" can be made. Corresponding to the afore-mentioned authors, zircon of this crystal morphology formed around 600 °C, a temperature that may be applied to the temperature regime in and around the Great Bavarian Quartz Lode "Pfahl" and wall rocks of the pegmatites (Figs. 1, 10a, b). Within the pegmatites, themselves, the zircon morphology is strikingly different from that of the Ti-bearing mineral aggregates. The morphological type is characterized by a lack of the prismatic faces {100} or by their reduction so that a bipyramidal crystal shape will result out of that. According to the above mentioned authors, the temperature of formation ranges from 500 to 600°°C (Fig. 10).

Monazite does not offer a similar variability in crystal morphology as its associate zircon in the stream sediments. The monazite crystal morphology encountered in the Deggendorf area is of the same type of morphology found in the Tittling granite emplaced further SE along the "Pfahl" (Fig. 1) (Dill et al., 2012b). The formation of the major shear zone, called "Pfahl", the emplacement of the granites and pegmatites in the southern area, and the nigrinisation are genetically linked with each other as they share the same environment of formation and physical–chemical regimes interlocked with each other.

5.3.6. Spinel group- and iron minerals

The spinel group minerals can be subdivided into three groups, using the trivalent cation as discriminator, the spinel series sensu stricto with Al, the magnetite series bearing Fe and the chromite series accommodating trivalent chromium (Deer et al., 1996). The first two groups are also found associated with "nigrine", although only in minor amounts.

The common spinel hercynite has been investigated from the crystallographic point of view by Kostov and Kostov (1999). Magnetite in "nigrine" only has elevated Ti and V contents and following the discrimination plots of Dupuis and Beaudoin (2011) we suggest derivation from a magmatic Fe–Ti–(V) mineralization, similar to those leading to those deposits which are still a relevant source of Fe, Ti and V worldwide (Dill, 2010). The anorogenic and/or extensional regime which the Fe–Ti–(V) deposits used to be correlated with has little meaning when it comes to the interpretation of the origin of magnetite in "nigrine". It is mainly the oxygen partial pressure that impacts on the presence or absence of ilmenite, hemo-ilmenite, titaniferous magnetite, magnetite and pyrrhotite or even rutile in these deposits. A low PO_2 causes titaniferous magnetite to evolve whereas an increasing PO_2 is conducive to titaniferous hematite. Type A "nigrine" formed at very low Eh << 0 with pyrrhotite (and little sphalerite). There is little trivalent Fe present in this Fe–Ti system, although rutile may be doped with ferric iron, involving substitution of Fe^{3+} onto octahedral Ti^{4+} sites and charge-balanced by oxygen vacancies (Bromiley and Hilaret, 2005). In type B "nigrine" an intermediate stage is attained with bivalent and trivalent Fe in magnetite, passing eventually into hematite. Type C is the most strongly oxidized member

Table 4
Correlation coefficients between TiO_2 in "nigrine" and "antinigrine" and associated elements in stream sediments of different types of colluvial, alluvial and fluvial deposits at the western edge of the Bohemian Massif (SE Germany). The distance between the nearest outcrop of phosphate pegmatite and each sampling site within the clastic aureole around this pegmatite is given in kilometers. Elements found within or at the margin of these phosphate pegmatites are highlighted as to whether these elements are positively correlated with TiO_2 (in black bold-faced characters) or negatively correlated (in red bold-faced characters). For example, away from pegmatites the correlation coefficient $R_{TiO2\ vs.\ Nb}$ diminishes from 0.92 to 0.42. Niobium is the only element of this kind reflecting a clearcut trend and as such qualifies as a proximity indicator—see also Fig. 4. The reader is referred to Table 2 for explanation of the environment of deposition and for a more detailed description to Fig. 5.

Sampling site	Deggendorf ("antinigrine")	Lerau ("nigrine+antinigrine")	Pleystein ("nigrine")	Plaumbach–Pingermühle ("nigrine")
Environment of deposition	colluvial–alluvial IIIb	fluvial IIIa	colluvial–alluvial fluvial IIIb–IIIa	fluvial IIIa
Types	A–B–C	A–B	A–B	A–B–C
Distance to pegmatite	<10 km	2 to 5 km	1 to 2 km	1 km
TiO_2	1.00	1.00	1.00	1.00
Al_2O_3	−0.96	−0.97	0.31	−0.02
Fe_2O_3	0.77	0.76	0.16	0.55
MnO	0.34	−0.98	0.85	0.59
MgO	−0.54	−0.98	0.28	0.10
CaO	−0.94	−0.97	0.24	0.26
Na_2O	−0.90	−0.71	−0.02	−0.04
K_2O	−0.91	−0.70	0.02	−0.01
P_2O_5	**−0.53**	**−0.89**	**−0.23**	**−0.20**
Ba	−0.90	−0.81	−0.25	0.12
Ce	−0.17	0.42	0.16	−0.23
Co	0.36	0.68	0.14	−0.02
Cr	0.41	0.66	0.04	−0.26
Cs	0.71	1.00	0.53	0.79
Cu	0.28	0.63	0.12	−0.14
La	−0.20	0.56	0.16	−0.24
Nb	0.42	0.77	0.85	0.92
Nd	−0.14	0.40	0.11	−0.26
Ni	−0.23	0.36	0.15	−0.08
Pb	−0.08	0.72	−0.23	−0.30
Rb	−0.68	−0.22	0.05	0.01
Sc	0.48	−0.89	0.44	0.27
Sm	0.19	n.d	n.d.	−0.11
Sn	0.59	0.77	0.42	0.69
Sr	−0.92	0.17	−0.26	0.21
Ta	0.24	0.83	0.62	0.82
Th	−0.18	0.39	0.24	−0.25
U	n.d.	−0.29	0.04	−0.19
V	0.31	0.31	0.40	0.33
W	0.77	0.78	0.27	0.79
Y	**−0.18**	**−0.96**	**0.23**	**−0.23**
Zn	0.37	0.47	0.27	−0.10
Zr	−0.30	0.11	0.19	−0.25
REE	**−0.16**	0.46	0.16	**−0.24**

n.d. = not determined.

of the "nigrine"-aggregates. By analogy with the classification scheme put forward by Ishihara and Wang (1999) for granitoids and by Meinert (1992) for skarn deposits a similar fourfold redox classification may be designed for the pegmatitic source area, with pyrrhotite marking the lowest level of Eh: (1) pyrrhotite-Eh << 0, (2) ilmenite-Eh < 0, (3) magnetite-Eh ≤ 0, (4) hematite-Eh > 0.

5.4. Secondary minerals and the physical–chemical regime during weathering and transport

5.4.1. Pseudorutile and "leucoxene"

Pseudorutile is present in the HM aggregates, whereas brookite or anatase, typical of supergene processes involving the migration of titaniferous solutions, are absent from "nigrine" as well as "antinigrine". Iron was not completely removed from the chemical system under study and the chemical regime affecting the proximal marker HM aggregates is held to be moderately oxidizing and acidic, otherwise the couple anatase and kaolinite should have been expected as elsewhere in the pervasively weathered crystalline basement rocks at the western edge of the Bohemian Massif. The transition of Fe–Ti minerals from HM aggregates into pseudorutile observed in the study area and the subsequent appearance of "leucoxene" made up of fine-grained anatase, brookite and goethite reflect a steady increase in the oxygen partial pressure, as the HM aggregates became fragmented along transport and eventually disintegrated into their components as reflected by the Ti/(Ti + Fe) ratios (ilmenite (<0.59) ⇒ pseudorutile (0.55 to 0.76) ⇒ anatase (1.00)) (Tables 2, 7) (Gilg and Frei, 1997; Grey and Reid, 1975; Kitagawa and Köster, 1991). Part of the pseudorutile in the "nigrine" compounds is a relic of alteration of primary Ti compounds in the source area, still preserved in the HM aggregates during weathering and transport. Pseudorutile does not qualify as a HM to survive long-distance fluvial transport (Dill, 2007). If ilmenite is present uncorroded, its long-lasting exposure during intensive chemical weathering can be excluded. The presence of bivalent Fe in ilmenite would cause ilmenite to be converted into Fe-deficient titaniferous compounds upon chemical weathering (Table 7). Rutile in "nigrine" has no meaning as a marker for the intensity of supergene alteration due to its high resistance to weathering that is only matched by zircon and tourmaline (Table 7).

5.4.2. Ti–Al–P–Fe compounds

Even if the precise mineralogical nature of these chemical compounds could not be determined during this study with EMPA, there is one thing for certain. Aluminum–iron phosphates formed during oxidizing conditions when goethite was stable. Both groups contain phosphorus and, consequently attest to Al- and Fe-bearing phosphate minerals similar to those met during the youngest stages of the pegmatitic mineralization (Dill et al., 2012a). Those mineral assemblages dominated by variscite and cacoxenite are indicative of pH values ≤4 (Dill et al., 2008c).

5.5. Resistance to weathering and the dispersion in the drainage system

The resistance to weathering and the intergrowth of the various mineral phases involved in the build-up of "nigrine" and "antinigrine" aggregates are the decisive parameters as to when and where the single HM grains and HM aggregates show up downstream in the different parts of the drainage system (Table 2).

The HM aggregates became important as "armored relics", with less resistant minerals such as wolframite s.s.s. and columbite group minerals being sheltered by the more resistant minerals rutile and ilmenite (Morton, 1984; Morton and Hallsworth, 1999; Nickel, 1973). Rutile, zircon and tourmaline are the protagonists among the ultrastable minerals known to be least susceptible to chemical weathering and, hence, found in almost all placer deposits, even minor components. Ilmenite, with bivalent Fe dominant in its lattice, is more susceptible to weathering than rutile, which me to a certain extent incorporate trivalent Fe, but may still survive a long-distance transport down to large inland lakes or even the sea where its grains may contribute to the build-up of titanium beach or coastal placer deposits (Dill, 2007). This is also underpinned by the distribution of "nigrine" and "antinigrine" aggregates in SE Germany.

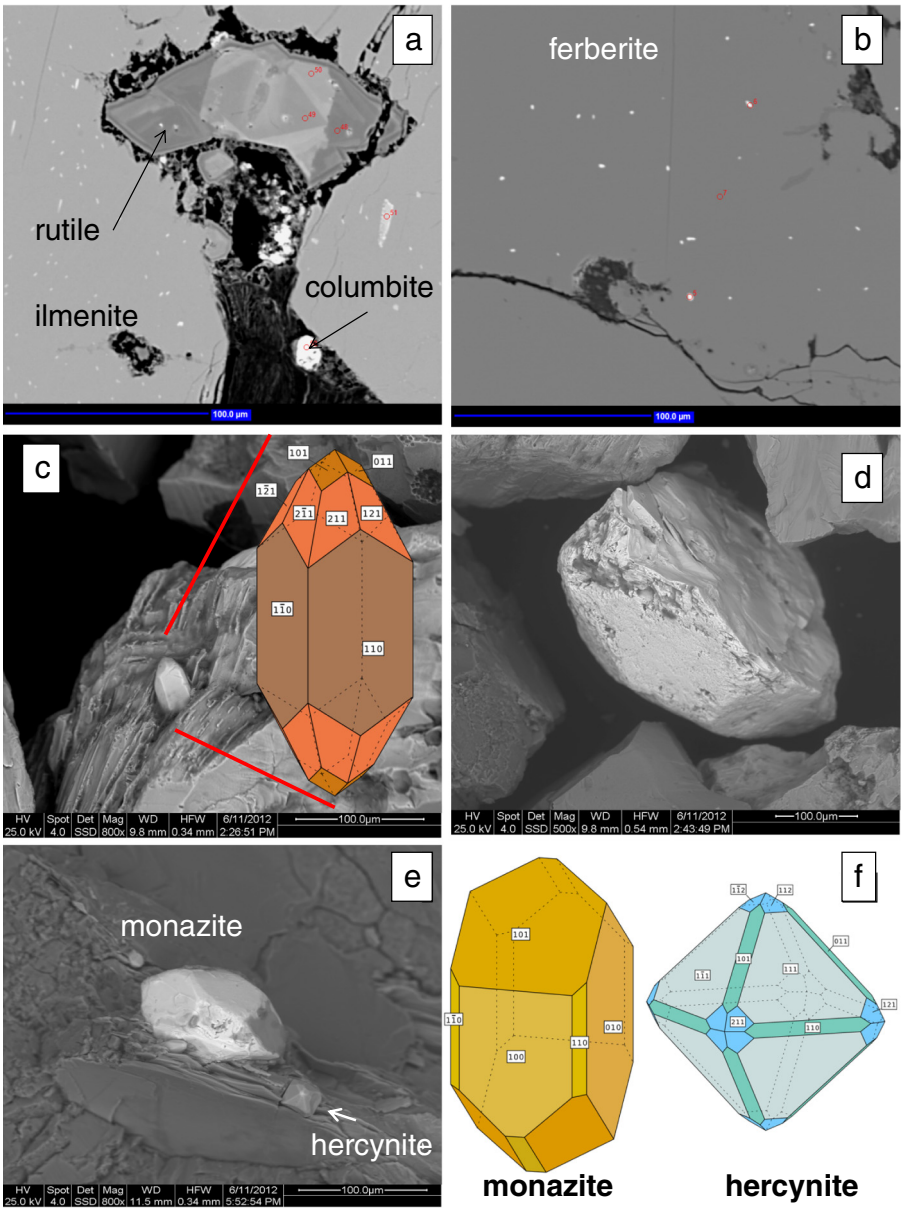

Fig. 8. Micrographs of accessory minerals in "nigrine" and "antinigrine".

a) Columbite-(Fe) in fissures of ilmenite together with zoned rutile. Red dots in the BSE images mark station points for EMPA (Deggendorf)(EPMA).
b) Fe-enriched wolframite (ferberite) disseminated within ilmenite. (Deggendorf)(EPMA).
c) Zircon in ilmenite. The zircon habit shows as characteristic crystal faces the prismatic faces (110) and the pyramid faces (211) as well as (110). (Deggendorf)(SEM).
d) Monazite besides ilmenite grains in stream sediments. It is a complex crystal broken apart on transport. (Deggendorf) (SEM).
e) Monazite crystal near hercynite (octahedra) in gneissic wall rocks of "nigrine" (Deggendorf) (SEM).
f) Idealized crystal morphologies of monazite and spinel on display in the SEM micrograph of Fig. 8e. Monazite demonstrates as a characteristic crystallographic feature the crystal habit face (101). Spinel (hercynite) has a rather complex morphology, as the common (111) faces are supplemented by subfaces (110) and (211).

The rutile-dominated HM aggregates occur down to the IIIa alluvial–fluvial placers, whereas the ilmenite-enriched HM aggregates only occur in the IIIb colluvial, alluvial and (fluvial) placers in the catchment area of drainage systems. Downstream of the IIIa drainage system "nigrine"-aggregates no longer occur. The reader is also referred to the alluvial, colluvial and fluvial placer deposits, of economic significance in Sierra Leone, Nigeria, Russia, DR Congo, Rwanda, Mozambique and Colombia, which were discussed in context with columbite in previous sections.

The heterogeneous titaniferous aggregates with fractures and growth failures get swiftly disintegrated into various components (Tables 2, 7). In terms of exploration these HM aggregates can only be used in the upper reaches of drainage systems, where artisanal mining is in some areas the only breadwinning process in Africa and South America. Due to the intimate intergrowth of rutile, ilmenite and a wealth of accessory minerals their value of a placer-deposit on its own is limited to the aforementioned areas and mining processes for element like Nb and Ta. Exploration geologists to be poised only for large-scale mining operations, will certainly head in search of Ti placers for down-stream placers either dominated by rutile or by ilmenite rather than for alluvial. fluvial "nigrine"-placers. The value of these HM aggregates lies exclusively within the field of exploration for primary targets.

The effect of post-depositional weathering altering HM assemblages of placer deposits has been discussed by Paine et al. (2005). According to their results, primary Fe–Ti minerals appear to have altered to secondary minerals, such as anatase and pseudorutile. By

Table 5
Chemical composition of accessory minerals in "nigrine" and "antinigrine", given in wt.%. Data are obtained from microprobe analyses. Some of the mineral compositions listed in this table are from the Hagendorf–Pleystein region (Dill et al., 2007b). The compounds FeO and Fe_2O_3 of pseudorutile and magnetite have been calculated based on the well-known chemical composition of Fe3O4 for magnetite while for pseudorutile this calculation was done based on a formula assumed to be $Fe_2Ti_3O_9$. Fe^{2+} und Fe^{3+} are both listed in the table for these minerals. Minerals of the pyrochlore group are calculated for 2 B cations (Nb + Ta + Ti + Mg + Si + Zr + Hf) owing to the crystal defects conducing to several vacancies in the lattice.

Location		Pingermühle (Zottbach)	Iglersreuth Tirschenreuth	Deggendorf	Deggendorf	Deggendorf	Pingermühle (Zottbach)	Pingermühle (Zottbach)	Pingermühle (Zottbach)	Deggendorf	Deggendorf	Deggendorf	Pingermühle (Zottbach)	Pingermühle (Zottbach)	Zollgraben	Iglersreuth Tirschenreuth
Mineral		Columbite	Columbite	Columbite	Columbite	Columbite	Pyrochlore	U-pyrochlore	Wolframite	Wolframite	Wolframite	Wolframite	Magnetite	Pseudorutile	Pseudorutile	Pseudorutile
Na_2O	wt.%							1.29								
MgO	wt.%	0.26	0.50						0.98	1.02	1.04	1.01	0.03	0.52	0.22	0.15
Al_2O_3	wt.%						0.03	0.10					0.02	0.07	0.09	0.03
SiO_2	wt.%						0.29	0.09		0.18	0.13	0.13		0.03	0.03	
CaO	wt.%						17.91	15.38								
Sc_2O_3	wt.%	1.07		1.79	1.57	1.43	0.03		0.15	0.14	0.14	0.12				
TiO_2	wt.%	5.96	8.19	6.10	5.49	5.36	5.12	17.26		6.38	2.73	4.91	3.22	57.56	59.01	57.62
V_2O_3	wt.%												0.17	0.28	0.32	0.29
Cr_2O_3	wt.%												0.03	0.03		
MnO	wt.%	3.54	2.43	1.21	1.16	1.28	0.16	0.09	1.72	2.58	2.47	2.47	0.09	1.14	2.44	3.64
FeO (total)	wt.%	16.89	17.93	17.94	18.31	19.50	1.37	0.68	24.28	24.08	22.51	23.21				
Fe_2O_3 (calc)	wt.%												62.56	41.12	38.56	37.00
FeO (calc)	wt.%												33.82	0.00	0.00	0.00
Nb_2O_5	wt.%	69.76	64.55	65.92	64.38	61.09	74.13	32.14	0.66	0.70	0.68	0.64		0.25	0.23	0.23
SnO_2	wt.%	0.14					0.05	0.29								
Ta_2O_5	wt.%	2.58	2.22	7.06	8.35	7.36	2.27	4.28								
WO_3	wt.%	0.69	4.71	2.39	2.14	2.72	0.40	0.60	70.43	66.79	71.46	69.93				
PbO	wt.%						0.30	1.00								
UO_2	wt.%						0.18	29.11								
Total	wt.%	100.89	100.53	102.41	101.40	98.74	102.24	102.31	98.22	101.87	101.16	102.42	99.95	101.00	100.90	98.96
Na	apfu	0.00	0.00	0.00	0.00	0.00	0.00	0.17	0.00	0.00	0.00	0.00	0.00	0.00	0.00	0.00
Mg	apfu	0.02	0.04	0.00	0.00	0.00	0.00	0.00	0.07	0.07	0.07	0.07	0.00	0.05	0.02	0.01
Al	apfu	0.00	0.00	0.00	0.00	0.00	0.00	0.01	0.00	0.00	0.00	0.00	0.00	0.01	0.01	0.00
Si	apfu	0.00	0.00	0.00	0.00	0.00	0.01	0.01	0.00	0.01	0.01	0.01	0.00	0.00	0.00	0.00
Ca	apfu	0.00	0.00	0.00	0.00	0.00	0.95	1.10	0.00	0.00	0.00	0.00	0.00	0.00	0.00	0.00
Sc	apfu	0.05	0.00	0.08	0.08	0.07			0.01	0.01	0.01	0.00	0.00	0.00	0.00	0.00
Ti	apfu	0.30	0.42	0.31	0.28	0.29	0.19	0.86	0.00	0.27	0.12	0.21	0.15	3.44	3.49	3.48
V	apfu	0.00	0.00	0.00	0.00	0.00			0.00	0.00	0.00	0.00	0.01	0.01	0.02	0.01
Cr	apfu	0.00	0.00	0.00	0.00	0.00			0.00	0.00	0.00	0.00	0.00	0.00	0.00	0.00
Mn	apfu	0.16	0.11	0.06	0.05	0.06	0.01	0.01	0.07	0.10	0.10	0.10	0.00	0.06	0.13	0.20
Fe (total)	apfu	0.76	0.81	0.81	0.84	0.93	0.11	0.08	1.03	0.90	0.89	0.88				
Fe3+ (calc)	apfu												1.81	2.06	1.93	1.89
Fe2+ (calc)	apfu												1.09	0.00	0.00	0.00
Nb	apfu	1.70	1.57	1.61	1.61	1.57	1.65	0.97	0.02	0.01	0.01	0.01	0.00	0.01	0.01	0.01
Sn	apfu	0.00	0.00	0.00	0.00	0.00	0.00	0.01	0.00	0.00	0.00	0.00	0.00	0.00	0.00	0.00
Ta	apfu	0.04	0.03	0.10	0.13	0.11	0.03	0.08	0.00	0.00	0.00	0.00	0.00	0.00	0.00	0.00
W	apfu	0.01	0.07	0.03	0.03	0.04	0.01	0.01	0.93	0.78	0.88	0.83	0.00	0.00	0.00	0.00
Pb	apfu	0.00	0.00	0.00	0.00	0.00	0.00	0.02	0.00	0.00	0.00	0.00	0.00	0.00	0.00	0.00
U	apfu	0.00	0.00	0.00	0.00	0.00	0.00	0.43	0.00	0.00	0.00	0.00	0.00	0.00	0.00	0.00
Total cations	apfu	3.05	3.05	3.01	3.02	3.07	2.96	3.74	2.12	2.14	2.09	2.11	3.00	5.08	5.07	5.09
Number of oxygen		6	6	6	6	6	[a]	[a]	4	4	4	4	4	9	9	9

[a] Calculated on the basis of 2 B-site cations.

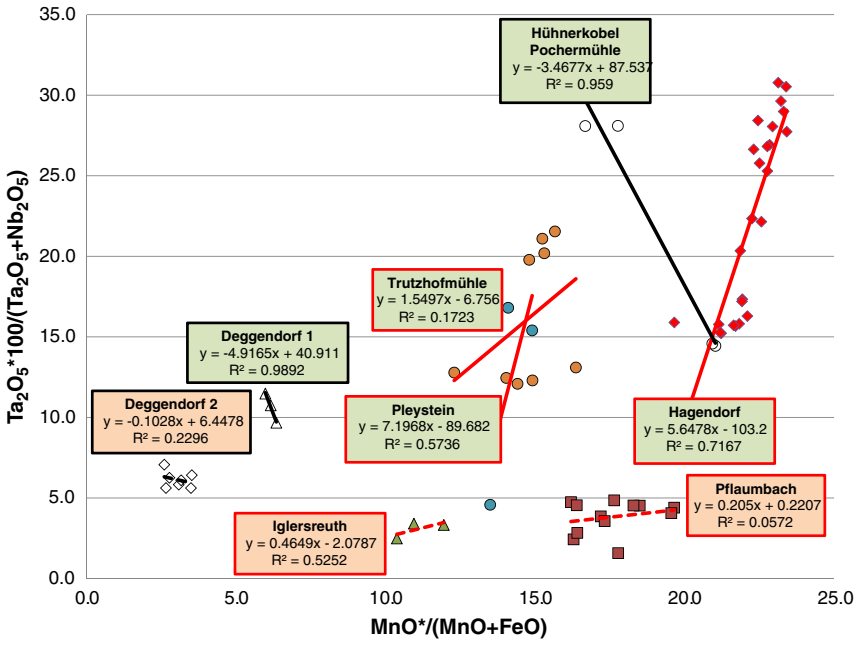

Fig. 9. X–y plot with MnO*/(MnO + FeO) vs. Ta_2O_5*100/(Ta_2O_5 + Nb_2O_5) to illustrate the chemical composition of columbite in "nigrine" and "antinigrine" (boxes in bright red) as well as in pegmatites and aplites from the study area (boxes in bright green). The frames colored in red and black are to correlate stream sediment-hosted and intrusion-hosted columbite. The equation in the various boxes describe the skewness of the trend lines provided as solid lines for pegmatites and aplites and expressed as ruled lines for columbite in stream sediments. (For interpretation of the references to color in this figure legend, the reader is referred to the web version of this article.)

analogy to primary minerals in the "armored relicts" these secondary minerals were denominated as "internal sediments" which formed upon transport and tell the researcher what the chemical regime of weathering was like (Table 7).

While attrition and chemical weathering grinds the existence of "nigrine" and "antinigrine" to a halt at the brink between IIIa and II drainage systems, columbite-(Fe) completely disappears only within the lower reaches of the II drainage systems. Thanks to the sheltering character of Ti minerals the clastic dispersion aureole around pegmatites is thereby widened by some orders of magnitude by the aforementioned transport-disintegration processes. Based upon the armored inclusions of columbite in nigrine, which get released from their carriers in the drainage system in class-II river systems after disintegration of the sheltering ilmenite–rutile intergrowth, the presence of rare-metal pegmatites in the catchment area may be predicted much earlier during stream sediment sampling than in drainage systems where columbite occurs only unsheltered in class-III alluvial–fluvial depositional environment proximal to the source area. In the absence of "nigrine" that plays the role of a carrier and protector, columbite would have already been decomposed within the class-III drainage systems and the dispersion aureole so vital for exploration would have significantly been narrowed down. Columbite's role is promote to a higher level and the mineral is cast thereby into the role of a distal marker mineral while "nigrine" and "antinigrine" aggregates, placed in the order of decreasing distance to the source, are cast as a proximal marker of rare-metal pegmatites (Tables 2, 7). This is also reflected by the decrease of the correlation coefficient $R_{Ti\ vs.\ Nb}$ as a function of distance from the pegmatite.

The HM aggregates were eroded from their crystalline source rocks and scattered in the different drainage system as early as 4.8 Ma following the age K/Ar dating of cryptomelane and U/Pb dating of secondary uranium minerals in the study area (Dill et al., 2010a,b) (Fig. 10d).

6. Synopsis and conclusions

"Nigrine" and "antinigrine" composed of rutile and ilmenite with or without accessory mineral phases are pegmatite-related in time and space, but they are not pegmatite-hosted Ti-enriched mineral aggregates (Table 1, Figs. 6, 8).

Table 6
Chemical composition of siliceous mineralization in shear zones at the western edge of the Bohemian Massif (SE Germany) and the more central parts of the Bohemian Massif (Czech Republic). The chemical composition is given in ppm and the mean temperature of formation was calculated according to the Ti-in-quartz geothermometer of Wark and Watson (2006).

Area	Li	Be	B	Mn	Ge	Rb	Sr	Sb	Al	P	K	Ti	Fe	Zn	Ga	Max (°C)	Mean (°C)	Min (°C)
SE Germany	4.56	0.08	14.34	0.58	0.94	0.17	0.14	0.05	839.37	0.00	4.42	78.62	10.24	3.92	0.27	730.9	719.2	707.7
	4.93	0.00	5.67	0.00	0.30	0.00	0.08	0.00	99.60	0.00	5.35	4.75	1.02	1.27	0.08	485.8	478.0	470.2
	5.52	0.00	28.99	0.25	0.75	0.01	0.24	0.08	569.21	0.21	4.53	71.06	9.09	3.78	0.22	719.3	707.9	696.6
Rozvadov	5.94	0.15	70.95	0.70	1.14	0.04	0.06	0.57	1223.39	1.73	11.69	150.36	31.24	1.89	0.19	811.8	798.8	785.9
Czech Republic	7.25	0.14	20.10	0.02	0.95	0.18	0.69	0.37	870.88	8.64	72.79	45.79	16.53	2.24	0.00	672.1	661.4	650.9
	8.59	0.22	33.00	7.30	1.21	0.58	0.34	0.67	1303.14	0.00	459.24	168.70	59.13	4.70	0.26	827.5	814.2	801.1
Ostruvek	24.15	0.17	1.65	0.37	0.76	0.00	0.24	0.18	551.56	0.00	10.43	32.45	7.18	5.24	0.26	638.1	628.0	618.0
Czech Republic	21.46	0.22	1.71	0.09	0.87	0.00	0.10	0.07	819.51	16.50	34.32	296.98	4.90	4.58	0.00	912.1	897.2	882.6
	26.12	0.35	0.97	4.03	0.87	0.03	0.43	0.07	1133.98	0.00	25.51	142.80	84.85	6.18	0.52	804.9	792.0	779.2
Jedlina	38.24	0.13	1.34	21.28	0.57	3.09	20.91	0.09	1271.38	0.00	129.66	2.25	58.87	7.52	0.00	439.6	432.5	425.4
Czech Republic	7.37	0.65	1.34	23.63	0.40	4.11	14.93	0.09	1381.00	2.14	732.15	2.37	41.29	9.65	0.00	442.6	435.4	428.3
	6.24	0.00	1.03	9.36	0.30	1.69	9.30	0.06	700.98	1.48	383.72	1.42	61.92	8.14	0.13	413.6	406.8	400.0
	11.83	0.00	0.52	3.45	0.34	0.64	3.56	0.16	932.95	9.97	331.99	2.17	357.62	7.39	0.04	437.4	430.2	423.1

Data obtained from laser-ablation inductively-coupled plasma mass spectrometry (LA-ICP-MS).

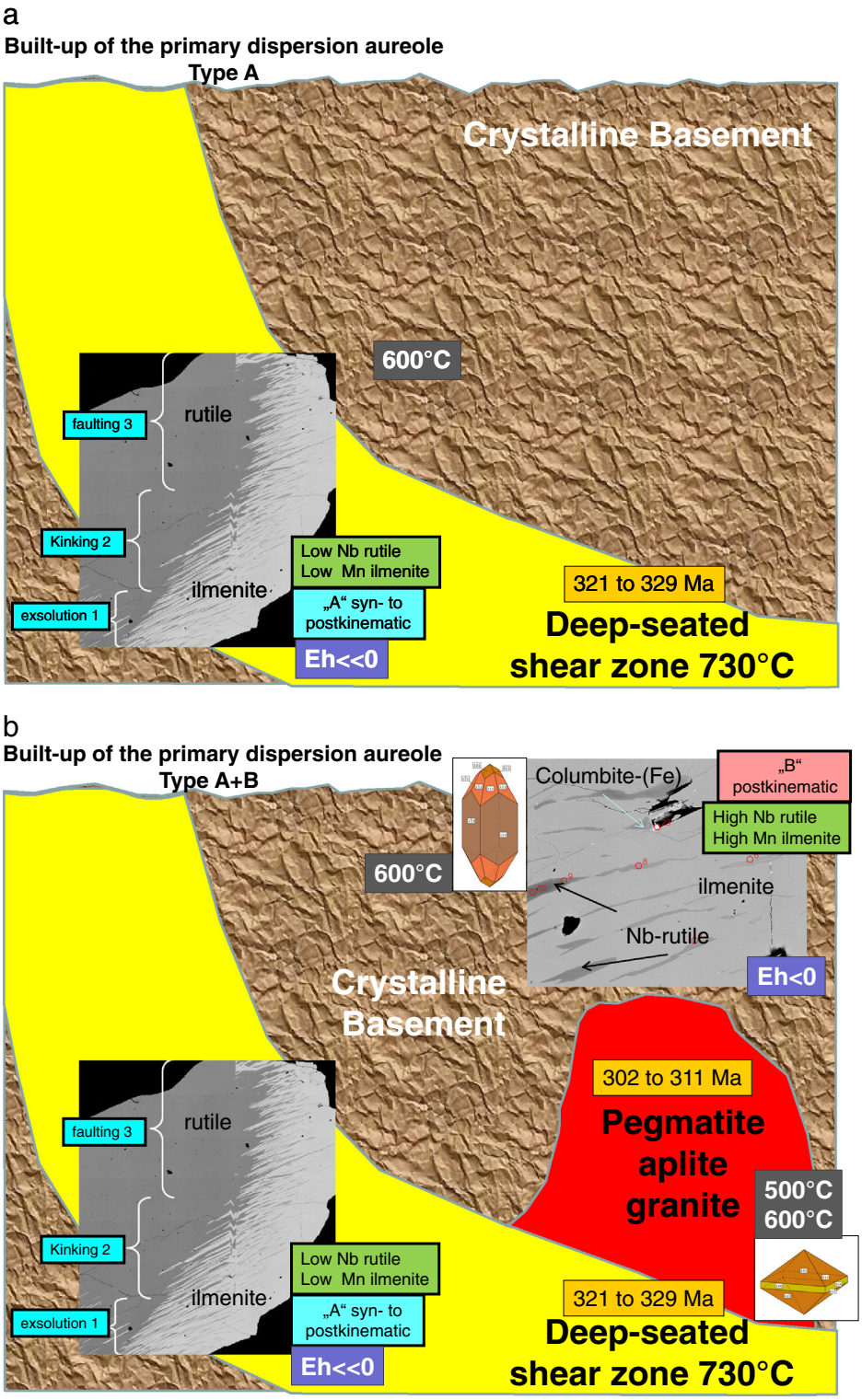

Fig. 10. Synoptical view of "nigrine/antinigrine" types in relation to the crystalline basement rocks and the pegmatitic intrusions. Each type is shown by a characteristic micrograph, the Eh value of the regime of formation is given in the purple box, the presence of the most diagnostic element Nb and Mn for each major mineral in the green box and structural setting in the red and bright blue boxes, respectively.

a) Type A developed along deep-seated lineamentary shear zones such as the Great Bavarian Quartz Lode also called "Pfahl" (Fig. 1). The micrograph shows the syn- to postkinematic nature of this Ti mineral aggregate. The onset shearing and mobilization took place between 321 and 329 Ma at a temperature of as much as 730 °C.
b) Type B developed in the wall and roof rocks of granites, pegmatites and aplites which were intruded between 302 and 311 Ma. The characteristic types of zircon morphology, useful as a geothermometer are given in a small cartoon together with the temperature of formation for the pegmatites and its wall rocks/roof rocks.
c) Type C developed near the granites and shear zones as part of a shallow shear zone hosted mineralization, the age of formation of which cannot clearly be constrained. The shear-zone-hosted mineralization faded out at 470 °C.
d) From the late Pliocene (<4.8 Ma) onward chemical weathering and erosion shaped the landscape of the NE Bavarian Basement and caused the titaniferous HM aggregates to be accumulated in creeks and rivulets of the class-III drainage systems (see also Table 2, Fig. 1b).

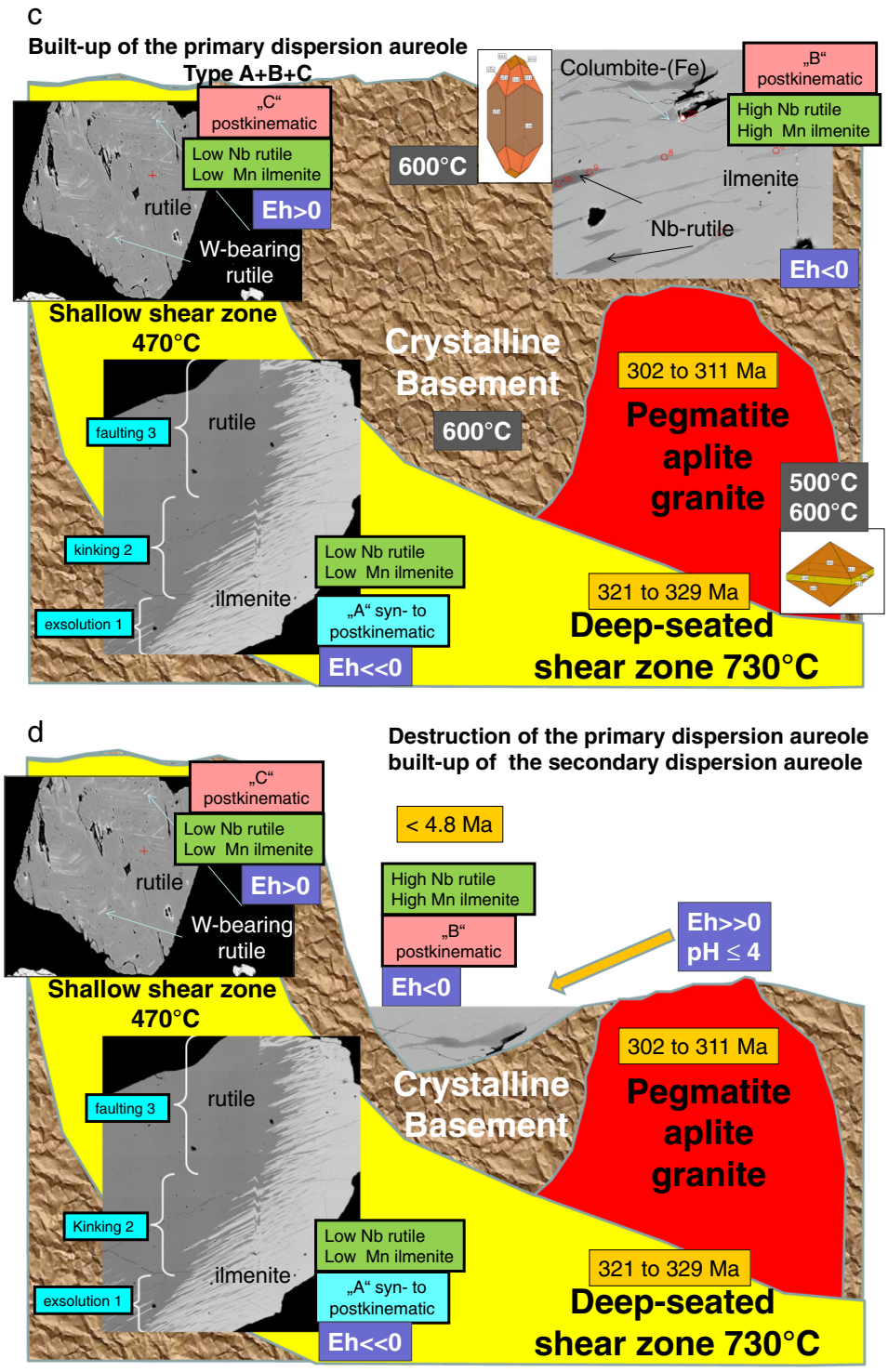

Fig. 10. (*continued*).

6.1. The origin of Ti-bearing mineral aggregates and the primary lithochemical dispersion aureole

The primary source of these titaniferous HM aggregates lies within the gneissic rocks of the crystalline basement proximal to or within shear zones filled with silica (Fig. 10). Moreover these sites are lined up along the boundary between the autochthonous basement rocks of the Moldanubicum and the allochthonous nappe of the Bohemicum (Teplá–Barrandian) (Fig. 1c). The Saxothuringian/Teplá–Barrandian convergence lasted from 380 to 346 Ma and terminated at 346 to 337 Ma by a rapid gravity-driven collapse of the thickened lithosphere (Hajná et al., 2012).

Nigrinisation is an alteration process exclusive to the gneissic country rocks and a mirror image of the state of fractionation.

Between 329 and 321 Ma the shear zone-related mobilization marked by the primitive Type A started around 730 °C at the western edge of the Bohemian Massif (Fig. 10a). It is present in all sites under study, excluding the northernmost study area at Iglersreuth, which reflects the shallowest part of the “nigrine” system, lacking any quartzose

Table 7
Mineralogy as a marker for the physical–chemical regime and the structural setting during formation and alteration of titaniferous HM aggregates "nigrine" and "antinigrine". The physical variation-transport (exploration) shows where and when HM or HM aggregates appear in the drainage systems. The chemical variation—secondary minerals (alteration) displays the marker minerals for the physical–chemical regime during chemical weathering, erosion and transport—see also Fig. 10d. The chemical variation—primary minerals (intrusion) displays the marker minerals for the physical–chemical regime during shear zone-related mobilization, wall rock alteration and the formation of the pegmatites—see also Fig. 10a, b, and c.

Physical and chemical alteration	Physical variation	Chemical variation		Chemical variation
Heavy minerals and heavy mineral aggregates	Transport (exploration)	Secondary minerals (alteration)		Primary minerals (intrusion)
Type A	Drainage system IIIb and IIIa			Pre- to synkinematic nigrinisation
Type B	Drainage system IIIb and IIIa			Early postkinematic nigrinisation
Type C	Drainage system IIIb and IIIa			late postkinematic nigrinisation
Ilmenite				Type A/C = fractionation of melt Type B = hydrothermal input of Mn
	Present in all classes of the drainage systems	Well-preserved grains: low oxygen fugacity	Eh <0	low oxygen fugacity Eh <0
Rutile	Present in all classes of the drainage systems			Type A/C = formation from mafic minerals/retrograde metamorphism and shearing Type B = related to mobilization of pegmatites/aplites by shearing
Columbite	Drainage system IIIb and IIIa (as armored relic) Drainage system III and II (after disintegration of HM aggregates) Decrease of $R_{Ti\ vs.\ Nb}$ as a function of distance from pegmatite			"Nigrine" in gneiss and quartz dykes are less strongly fractionated than pegmatites and aplites.
Pyrochlore	Absent from stream sediments			Waning heat event of the Variscides
Wolframite	Absent from stream sediments			Postkinematic nigrinisation hydrothermal mineralization
Monazite–xenotime	Present in all classes of the drainage systems			Morphological type of monazite = granite-related
Zircon	Present in all classes of the drainage systems			Stubby prismatic type of zircon = 600 °C temperature in the shear zone environment Bi-pyramidal type of zircon = 500 °C to 600 °C temperature in the pegmatite
Pyrrhotite–sphalerite	Absent from stream sediments			Type A = strongly reducing environment Eh <<0
Hercynite–magnetite	Present in all classes of the drainage systems			Type B = intermediate redox state Eh ≤ {111} >> {110} habit = high-temperature
Hematite	Present in all classes of the drainage systems	Oxidation during weathering		Type B = strongly oxidizing (only in parts, e.g., fissures) Eh >0
Pseudorutile	Absent from stream sediments	Rising oxygen fugacity under supergene conditions	Eh ≤0	
	Anatase, brookite and goethite ("leucoxene") Drainage system IIIa after disintegration of HM aggregates	Most elevated level of oxygen fugacity under supergene conditions	Eh >0	
Ti–Al–P–Fe compounds	Absent from stream sediments	Eh >0	pH ≤4	
Nb–Ti–Ta–P compounds	Absent from stream sediments	Eh >0	pH <7 (?)	

shear zones as in the south. Type A denotes the most primitive stage with respect to fractionation and proximal to the locus of mobilization along the shear zone (Table 7).

Emplacement of pegmatite was accompanied by the more complex type B, abundant in Nb, between 500 and 600 °C (Fig. 10b). Mobilization of the alkaline melt commenced 311 Ma ago and faded out around 302 Ma. Type B reflects the most advanced level of fractionation at a more distal position relative to the shear zone but at a more proximal position relative to the present-day loci of pegmatites and aplites enriched in rare metals, prevalently niobium.

At shallow depth, within the shear zones, W-bearing type C developed around 400 °C (Fig. 10c). Type C still reflecting the granitic affiliation by its Nb and W contents is the youngest type of Ti mobilization. It may be found in space with the shear zone but not in time with the shearing process along which the mobilization of the pegmatitic and aplitic intrusions began.

"Nigrine" and "antinigrine" are located within the country/roof rocks of the pegmatites. They form part of the primary dispersion aureole around pegmatites within the crystalline rocks and can be considered as a lithochemical tool for hidden pegmatite deposits, with type B "nigrine" developing most proximal to Nb-bearing pegmatites.

The secondary aureole of dispersion developed when the channels of the modern drainage system cut into the primary dispersion aureole surrounding the pegmatites. As a consequence of this erosional process, Ti-bearing HM aggregates including their accessory minerals got released from their source and became a tool to track down the pegmatites in the catchment area of drainage systems.

"Nigrine" and "antinigrine" are proximity indicators being located most proximal to the pegmatitic target. Columbite-(Fe) is a proximity indicator efficacious at a more distal position, which comes into effect only when the "armored relics" and Ti-bearing HM aggregates were destroyed on transport. The HM aggregates act as a shelter and, thereby, enlarge the mechanical dispersion aureole around pegmatites by some orders of magnitude (Tables 2, 4, Fig. 1). If columbite-(Fe) had to travel freely in the alluvial–fluvial drainage systems its transport range would be confined to less than 2 km around the pegmatite leaving little chance to localize the pegmatite.

6.2. Denudation of Ti-bearing mineral aggregates and the secondary dispersion aureole

During the Neogene erosion and chemical weathering provoked the release of the marker HM aggregates from their source rocks and gave rise to the mechanical dispersion aureole around the pegmatites which can be used for targeting upon them during exploration (Fig. 10d).

Secondary minerals forming an "internal sediment" within the titaniferous HM aggregates tell us the story about the supergene alteration during erosion and transport. They are of minor value as an ore guide but of assistance to geomorphologists and geologists studying the most recent part of the Earth's history.

The Nb-, Ta-, Mn- and Fe contents in these titaniferous HM aggregates, the variegated spectrum of mineral inclusions and the crystal morphology of some of the accessory minerals predict what type of pegmatite one may expect at outcrop in the upper reaches of the drainage system or as blind ore body underneath the roof rocks.

Titaniferous HM aggregates are suitable ore guides to highly fractionated intrusive rocks such as aplites and pegmatites. Even though many of the deposits in Central Europe are now mined out or no longer may be denominated as deposits by world standard, they may contribute to the exploration of hidden ore deposits in older terrains elsewhere in the world. In Western Australia the Li–Sn–Ta pegmatite at Greenbushes which is of Archaean age was intruded and crystallized synchronously with deformation in a medium- to high-temperature and medium-pressure metamorphic setting (Partington et al., 1998). Deep-seated shear zones rather than granites nearby are of major control as it is the case with the much younger Variscan pegmatites in during this study. The rare-element bearing Tanco pegmatite, Canada, may be another example of the same as the Volta Grande pegmatite in Brazil which is more of importance for its Li and Rb contents (Černý, 2005; Quéméneur and Lagache, 1994).

In the study area three new discoveries, one containing Sc in some minerals hitherto no found elsewhere in the world (under detailed study) and another abundant in lazulite (Dill et al., 2008a, 2012b). The third one is under mineralogical investigation.

"Nigrine" and "antinigrine" do not form part of the mineral assemblage of the pegmatites, proper, although they host minerals typical of these felsic intrusive rocks such as columbite-(Fe). Both Ti compounds mentioned above are genetically related to the emplacement of the pegmatites but they reside as concretions or dissemination in the crystalline wall and roof rocks of the pegmatites which were truncated much earlier by erosion and delivering debris to the stream sediments in the various drainage system, than the pegmatite underneath. These titaniferous debris and their mineral inclusions can thus be taken as an ore guide to the blind pegmatitic ore body.

The titanium minerals have no economic potential as placer-type minerals of their own as far as industrial mining in rivers and along beaches are concerned, due to the intimate intergrowth of rutile, ilmenite and accessory minerals. Only in Africa, e.g., Sierra Leone and South America, e.g., Colombia some of these placer minerals, won by artisanal miners, can be sold for a profit for their Ta contents.

The common types of "nigrine" and "antinigrine" are intermediate repositories on the way to build up of Ti placer deposits downstream of class-III drainage systems, in fluvial, nearshore lacustrine and nearshore marine depositional environments where either rutile or ilmenite are the principal minerals of interest—overview see in Dill (2010).

Acknowledgments

We are indebted to F. Korte who conducted the chemical analyses in the laboratory of BGR. The preparation of samples and SEM analyses were performed by I. Bitz and D. Klosa. D. Weck has carried out the XRD analyses. ICP-MS analyses of quartz were performed in the laboratories of the Geological Survey of Norway. We extend our gratitude to three anonymous reviewers who spent their time reviewing our paper for *Ore Geology Reviews*. We express also our thanks to Franco Pirajno, editor-in-chief of *Ore Geology Reviews* for his editorial handling of our paper.

References

Abella, P.A., Cordomí, M.C., Melgarejo Draper, J.C., 1995. Nb–Ta-minerals from the Cap de Creus pegmatite field, eastern Pyrenees: distribution and geochemical trends. Mineral. Petrol. 55, 53–69.

Aleksandrov, V.B., 1963. Isomorphism of cations in titaniferous tantalo-niobates of composition AB2X6. Dokl. Akad. Nauk 153, 672–675 (English translation 129–131).

Anderson, S.D., Černý, P., Halden, N.M., Chapman, R., Uher, P., 1998. The YITT-B pegmatite swarm at Bernic Lake, southeastern Manitoba: a geochemical and paragenetic anomaly. Can. Mineral. 36, 283–301.

Antunes, I.M.H.R., Neiva, A.M.R., Silva, M.M.V.G., 2002. The mineralized veins and the impact of old mine workings on the environment at Segura, central Portugal. Chem. Geol. 190, 417–431.

Atencio, D., Andrade, M.B., Christy, A.G., Gieré, R., Kartashov, P.M., 2010. The pyrochlore supergroup of minerals: nomenclature. Can. Mineral. 48, 673–698.

Benisek, A., Finger, F., 1993. Factors controlling the development of prism faces in granite zircons: a microprobe study. Contrib. Miner. Petrol. 114, 441–451.

Bingen, B., Davis, W.J., Austrheim, H., 2001. Zircon U–Pb geochronology in the Bergen arc eclogites and their Proterozoic protoliths, and implications for the pre-Scandian evolution of the Caledonides in western Norway. Geol. Soc. Am. Bull. 113, 640–649.

Borger, H., Burger, D., Kubiniok, J., 1993. Verwitterungsprozesse und deren Wandel im Zeitraum Tertiär–Quartär. Z. Geomorphol. N.F. 37, 129–143.

Bromiley, G., Hilaret, N., 2005. Hydrogen and minor element incorporation in synthetic rutile. Mineral. Mag. 69, 345–358.

Černý, P., 1989. Exploration strategy and methods for pegmatite deposits of tantalum. In: Möller, P., Černý, P., Saupé, F. (Eds.), Lanthanides, Tantalum and Niobium. Springer-Verlag, Berlin, Germany, pp. 271–299.

Černý, P., 2005. The Tanco rare-element pegmatite deposit, Manitoba: regional context, internal anatomy, and global comparisons. In: Linnen, R.L., Samson, I.M. (Eds.), Rare-element geochemistry and mineral deposits. Geol. Assoc. Can., Short Course Notes, 17, pp. 127–158.

Černý, P., Chapman, R., Simmons, W.B., Chackowsky, E., 1999. Niobian rutile from the McGuire granitic pegmatite, Park County, Colorado: solid solution, exsolution, and oxidation. Am. Mineral. 84, 754–763.

Černý, P., Novák, M., Chapman, R., Masau, M., 2000. Two-stage exsolution of a titanium $(Sc, Fe^{3+})(Nb, Ta)O4$ phase in Norwegian niobian rutile. Can. Mineral. 38, 907–913.

Černý, P., Novák, M., Chapman, R., Ferreira, K.J., 2007. Subsolidus behavior of niobian rutile from the Písek region, Czech Republic: a model for exsolution in W- and $Fe^{2+} >> Fe^{3+}$-rich phases. J. Geosci. 52, 143–159.

Clemens, J., 1998. Observations on the origins and ascent mechanisms of granitic magmas. J. Geol. Soc. Lond. 155, 843–851.

Deer, W.A., Howie, R.A., Zussman, J., 1996. An Introduction to the Rock-Forming Minerals, 2nd edition. Prentice Hall (712 pp.).

Dill, H.G., 1989. Metallogenetic and geodynamic evolution in the Central European Variscides—a pre-well site study for the German Continental Deep Drilling Programme. Ore Geol. Rev. 4, 279–304.

Dill, H.G., 2007. Grain morphology of heavy minerals from marine and continental placer deposits, with special reference to Fe–Ti oxides. Sediment. Geol. 198, 1–27.

Dill, H.G., 2010. The "chessboard" classification scheme of mineral deposits: Mineralogy and geology from aluminum to zirconium. Earth Sci. Rev. 100, 1–420.

Dill, H.G., Melcher, F., Fuessl, M., Weber, B., 2006. Accessory minerals in cassiterite: a tool for provenance and environmental analyses of colluvial–fluvial placer deposits (NE Bavaria, Germany). Sediment. Geol. 191, 171–189.

Dill, H.G., Gerdes, A., Weber, B., 2007a. Cu–Fe–U phosphate mineralization of the Hagendorf–Pleystein pegmatite province, Germany: with special reference to Laser-Ablation-Inductive-Coupled-Plasma Mass Spectrometry (LA-ICP-MS) of iron-cored torbernite. Mineral. Mag. 71, 423–439.

Dill, H.G., Melcher, F., Fuessl, M., Weber, B., 2007b. The origin of rutile–ilmenite aggregates ("nigrine") in alluvial–fluvial placers of the Hagendorf pegmatite province, NE Bavaria, Germany. Mineral. Petrol. 89, 133–158.

Dill, H.G., Techmer, A., Weber, B., Fuessl, M., 2008a. Mineralogical and chemical distribution patterns of placers and ferricretes in Quaternary sediments in SE Germany: the impact of nature and man on the unroofing of pegmatites. J. Geochem. Explor. 96, 1–24.

Dill, H.G., Melcher, F., Gerdes, A., Weber, B., 2008b. The origin and zoning of hypogene and supergene Fe–Mn–Mg–Sc–U–REE–Zn phosphate mineralization from the newly discovered Trutzhofmühle aplite (Hagendorf pegmatite province, Germany). Can. Mineral. 46, 1131–1157.

Dill, H.G., Weber, B., Gerdes, A., Melcher, F., 2008c. The Fe–Mn phosphate aplite "Silbergrube" near Waidhaus, Germany: Epithermal phosphate mineralization in the Hagendorf–Pleystein pegmatite province. Mineral. Mag. 72, 1143–1168.

Dill, H.G., Hansen, B., Keck, E., Weber, B., 2010a. Cryptomelane a tool to determine the age and the physical–chemical regime of a Plio-Pleistocene weathering zone in a granitic terrain (Hagendorf, SE Germany). Geomorphology 121, 370–377.

Dill, H.G., Gerdes, A., Weber, B., 2010b. Age and mineralogy of supergene uranium minerals—tools to unravel geomorphological and palaeohydrological processes in granitic terrains (Bohemian Massif, SE Germany). Geomorphology 117, 44–65.

Dill, H.G., Weber, B., Botz, R., 2011. The baryte-bearing beryl-phosphate pegmatite Plössberg—a missing link between pegmatitic and vein-type barium mineralization in NE Bavaria, Germany. Geochemistry 71, 377–387.

Dill, H.G., Skoda, R., Weber, B., Berner, Z., Müller, A., Bakker, R.J., 2012a. A newly-discovered swarm of shearzone-hosted Bi–As–Fe–Mg–P aplites and pegmatites in the Hagendorf–Pleystein Pegmatite Province, SE Germany: a step closer to the metamorphic root of pegmatites. Canadian Minerologist Special Volume dedicated to Petr Černý, 50, pp. 943–974.

Dill, H.G., Weber, B., Klosa, D., 2012b. Crystal morphology and mineral chemistry of monazite–zircon mineral assemblages in continental placer deposits (SE Germany): ore guide and provenance marker. J. Geochem. Explor. 112, 322–346.

Drew, L.J., Qingrun, M., Weijun, S., 1990. The Bayan Obo iron–rare earth–niobium deposits, Inner Mongolia, China. Lithos 26, 46–65.

Duk-Rodkin, A., Barendregt, R.W., White, J.M., Singhroy, V.H., 2001. Geological evolution of the Yukon River: implications for placer gold. Quat. Int. 82, 5–31.

Dupuis, C., Beaudoin, G., 2011. Discriminant diagrams for iron oxide trace element fingerprinting of mineral deposit types. Miner. Deposita 46, 319–335.

Ercit, T.S., 2005. REE-enriched granitic pegmatites. In: Linnen, R.L., Samson, I.M. (Eds.), Rare-Element Geochemistry and Mineral Deposits. Geol. Assoc. Can., Short Course Notes, 17, pp. 175–199.

Feenstra, A., Peters, T., 1996. Experimental determination of activities in $FeTiO_3$–$MnTiO_3$ ilmenite solid solutions by redox reversal. Contrib. Mineral. Petrol. 126, 109–120.

Flem, B., Larsen, R.B., Grimstvedt, A., Mansfeld, J., 2002. In situ analysis of trace elements in quartz by using laser ablation inductively coupled plasma mass spectrometry. Chem. Geol. 182, 237–247.

Fletcher, W.K., 1997. Stream sediment geochemistry in today's exploration world. In: Gubins, A.G. (Ed.), Proceeding of exploration 97: Fourth Decennial International Conference on Mineral exploration, pp. 249–260.

Franke, W., 1989. The geological framework of the KTB drill site, Oberpfalz. In: Emmermann, R., Wohlenberg, J. (Eds.), The German Continental Deep Drilling Program (KTB). Springer, Heidelberg, Berlin, New York, pp. 37–54.

Frost, M.T., Grey, I.E., Harrowfield, I.R., Mason, K., 1983. The dependence of alumina and silica contents on the extent of alteration of weathered ilmenites from Western Australia. Mineral. Mag. 47, 201–208.

Gilg, H.A., Frei, R., 1997. Isotope dating of residual kaolin deposits in Europe (Tirschenreuth, Germany and St. Yrieix, France). In: Rongfu, P. (Ed.), Energy and mineral resources for the 21th century, geology of mineral deposits, mineral economics. Proceedings of the 30th International Geological Congress, Beijing, vol. 9. VSP International Science Publisher, Zeist, Netherlands, pp. 123–132.

Graham, J., Morris, R.C., 1973. Tungsten- and antimony substituted rutile. Mineral. Mag. 39, 470–473.

Grey, I.E., Reid, A.F., 1975. The structure of pseudorutile and its role in the natural alteration of ilmenite. Am. Mineral. 60, 898–906.

Grey, I.E., Watts, J.A., Bayliss, P., 1994. Mineralogical nomenclature: pseudorutile revalidated and neotype given. Mineral. Mag. 58, 597–600.

Hajná, J., Žák, J., Kachlık, V., Chadima, M., 2012. Deciphering the Variscan tectonothermal overprint and deformation partitioning in the Cadomian basement of the Tepla'–Barrandian unit, Bohemian Massif. Int. J. Earth Sci. 101, 1855–1873.

Hogarth, D., 1977. Classification and nomenclature of pyrochlore group. Am. Mineral. 62, 403–410.

Hou, B., Keeling, J., Frakes, L., Alley, N., Luo, X., 2008. Evolution and exploration of palaeochannels/palaeoshorelines, South Australia: a decade on—MRD-12 Fluvial palaeo-systems: evolution and mineral deposits. International Geological Congress, 2008, Oslo.

Illenberger, W., 1991. Pebble shape (and size !). J. Sediment. Petrol. 61, 756–767.

Ishihara, S., Wang, P.A., 1999. The ilmenite-series and magnetite series classification of Yanshanian granitoids of South China. Bull. Geol. Surv. Jpn. 50, 661–670.

Kitagawa, R., Köster, H.M., 1991. Genesis of the Tirschenreuth kaolin deposit in Germany compared with the Kohdachi kaolin deposit in Japan. Clay Miner. 26, 61–79.

Klinger, R., Sperling, T., 2008. Neue Ansätze zur Quantifizierung von Laserablation-ICP-MS-Analysen: Grundlagen und Anwendung auf Columbite. Geol. Bavarica 108, 392–416.

Komov, I.L., Lukashev, A.N., Koplus, A.V., 1994. Geochemical methods of prospecting for non-metallic minerals, VSP (400 pp.).

Kostov, I., Kostov, R.I., 1999. Crystal habits of minerals. Bulgarian Academic Monographs, pp. 1–415.

Lalomov, A., Bochneva, A., 2008. Heavy mineral placers of fluvial–lacustrine Oligocene paleosystem of West Siberia plain MRD-12 Fluvial palaeo-systems: Evolution and mineral deposits. International Geological Congress, 2008, Oslo.

Levinson, A.A., 1974. Introduction to Exploration Geochemistry. Applied Publishing Ltd., Maywood (624 pp.).

Linnen, R.L., Keppler, H., 1997. Columbite solubility in granitic melts: Consequences for the enrichment and fractionation of Nb and Ta in the Earth's crust. Contrib. Mineral. Petrol. 128, 213–227.

London, D., 2005. Granitic pegmatites: an assessment of current concepts and directions for the future. Lithos 80, 281–303.

Meinert, L.D., 1992. Skarn and skarn deposit. Geosci. Can. 19, 145–162.

Melcher, F., Sitnikova, M.A., Graupner, T., Martin, N., Oberthür, T., Henjes-Kunst, F., Gäbler, E., Gerdes, A., Brätz, H., Davis, D.W., Dewaele, S., 2008. Fingerprinting of conflict minerals: columbite–tantalite ("coltan") ores. SGA News 23, 1–14.

Melleton, J., Gloaguen, E., Frei, D., Novák, M., Breiter, K., 2012. How are the emplacement of rare-element pegmatites, regional metamorphism and magmatism interrelated in the Moldanubian domain of the Variscan Bohemian Massif, Czech Republic ? Can. Mineral. 50, 1751–1773.

Miall, A.D., 2006. The geology of fluvial deposits: sedimentary facies, basin analysis, and petroleum geology, 3rd edition. Springer (New York, Berlin, Heidelberg 582 pp.).

Morton, A.C., 1984. Stability of detrital heavy-minerals in Tertiary Sandstones from the North Sea Basin. Clay Miner. 19, 287–308.

Morton, A.C., 1991. Geochemical studies of detrital heavy minerals and their application to provenance research. In: Morton, A.C., Todd, S.P., Haughton, P.D.W. (Eds.), Developments in sedimentary provenance studies. Geological Society London Special Publication, 57, pp. 31–46.

Morton, A.C., Hallsworth, C.R., 1999. Processes controlling the composition of heavy mineral assemblages in sandstones. Sediment. Geol. 124, 3–29.

Mücke, A., Bhadra Chaudhuri, J.N., 1991. The continuous alteration of ilmenite through pseudorutile to leucoxene. Ore Geol. Rev. 6, 25–44.

Mücke, A., Keck, E., 2008. Untersuchungen an Columbiten (Fe, Mn) $(Nb, Ta)_2O_6$ und dem mit Columbit verwachsenen Neufund Petscheckit U (Fe, Mn) $(Nb, Ta)_2O_8$ aus dem Pegmatit von Hagendorf-Süd/Oberpfalz. Aufschluss 59, 373–392.

Müller, G., 1966. Die Beziehungen zwischen der chemischen Zusammensetzung, Lichtbrechung und Dichte einiger koexistiernder Biotite, Muskowite und Chlorite aus granitischen Tiefengesteinen. Contrib. Mineral. Petrol. 36, 659–672.

Nickel, E., 1973. Experimental dissolution of light and heavy-minerals in comparison with weathering and intrastratal solution. Contrib. Sedimentol. 1, 1–68.

Nickel, E., Nichols, M., 2004. Mineral names, redefinitions & discreditations passed by the CNMMN of the IMA. http://www.materialsdata.com.

Novák, M., Černý, P., 1998. Niobium–tantalum oxide minerals from complex granitic pegmatites in the Moldanubicum, Czech Republic; primary versus secondary compositional trends. Can. Mineral. 36, 659–672.

Novák, M., Černý, P., 2001. Distinctive compositional trends in columbite–tantalite from two segments of the lepidolite pegmatite at Rozná, western Moravia, Czech Republic. J. Czech Geol. Soc. 46, 1–8.

Novák, M., Černý, P., Uher, P., 2003. Extreme variation and apparent reversal of Nb–Ta fractionation in columbite-group minerals from the Scheibengraben beryl-columbite granite pegmatite, Marsikov, Czech Republic. Eur. J. Mineral. 15, 565–574.

Paine, M.D., Anand, R.R., Aspandiar, M., Fitzpatrick, R.R., Verrall, M.R., 2005. Quantitative heavy-mineral analysis of a Pliocene beach placer deposit in Southeastern Australia Using the AutoGeoSEM. J. Sediment. Res. 75, 742–759.

Partington, G.A., McNaughton, N.J., Williams, I.S., 1998. A review of the geology, mineralization, and geochronology of the Greenbushes Pegmatite, Western Australia. Econ. Geol. 90, 616–635.

Peters, W.C., 1987. Exploration and Mining Geology, 2nd edition. John Wiley and Sons Inc., New York (720 pp.).

Pettijohn, F.J., Potter, P.E., Siever, R., 1973. Sand and Sandstone. Springer, New York, Heidelberg (618 pp.).

Pupin, J.P., 1980. Zircon and granite petrology. Contrib. Mineral. Petrol. 73, 207–220.

Quéméneur, J., Lagache, M., 1994. La holmquistite des pegmatites de Volta Grande pres de São João Del Rei, Minas Gerais, Bresil: Caracteristiques chimiques et mineralogiques. Geonomos 2, 15–21.

Ramdohr, P., 1975. Die Erzmineralien und ihre Verwachsungen. Akademie-Verlag, Berlin (1277 pp.).

Rammelsberg, C.F., 1860. Handbuch der Mineralchemie. Engelmann, Leipzig (1039 pp.).

Sakoma, E.M., Martin, R.E., 2002. Oxidation-induced postmagmatic modifications of primary ilmenite, NYG-related aplite dyke, Tibchi Complex, Kalato, Nigeria. Mineral. Mag. 66, 591–604.

Seltmann, R., Faragher, A.E., 1994. Collisional orogens and their related metallogeney—a preface. In: Seltmann, R., Kämpf, H., Möller, P. (Eds.), Metallogeny of Collision Orogen. Czech Geological Survey, Prague, pp. 7–19.

Siebel, W., Thiel, M., Chen, F., 2006. Zircon geochronology and compositional record of late- to post-kinematic granitoids associated with the Bavarian Pfahl zone (Bavarian Forest). Mineral. Petrol. 86, 45–62.

Siegfried, P., 2008. Heavy mineral sand placer deposits of the Somaliland coast—interaction of fluvial, aeolian and marine processes MRD-12 Fluvial palaeo-systems: Evolution and mineral deposits. International Geological Congress, 2008, Oslo.

Smith, D.C., Perseil, E.A., 1997. Sb-rich rutile in the manganese concentrations at St. Marcel-Praborna, Aosta Valley, Italy: petrology and crystal chemistry. Mineral. Mag. 61, 655–669.

Stütz, A., 1799. Physikalisch-mineralogische Beschreibung des berühmten Gold- und Silberbergwerks bei Nagy-Ag in Siebenbürgen. Neues Schriftenr. Ges. Naturforsch. Freunde Berlin 2, 1–96.

Sweetapple, M.T., Collins, P.L.F., 2002. Genetic framework for the classification and distribution of archaean rare metal pegmatites in the North Pilbara Craton, Western Australia. Econ. Geol. 97, 873–895.

Tucker, M.E., 2001. Sedimentary petrology. Blackwell, Oxford (262 pp.).

Urban, A.J., Hoskins, B.F., Grey, I.E., 1992. Characterization of V–Sb–W-bearing rutile from the Hemlo gold deposit, Ontario. Can. Mineral. 30, 319-226.

Von Raumer, J.F., Stampfli, G.M., Bussy, F., 2003. Gondwana-derived microcontinents—the constituents of the Variscan and alpine collision orogens. Tectonophysics 365, 7–22.

Walravens, H., 2006. Julius Klaproth. His life and works with special emphasis on Japan. Jpn. Humboldtiana 10, 177–191.

Warenborgh, J.C., Figueiras, J., Mateus, A., Concalves, M., 2002. Nature and mechanism of ilmenite alteration; a Mossbauer and X-ray diffraction study of oxidized ilmenite from the Beja-Acebuches ophiolite complex (SE Portugal). Mineral. Mag. 66, 421–430.

Wark, D.A., Watson, E.B., 2006. TitaniQ: a titanium-in-quartz geothermometer. Contrib. Mineral. Petrol. 152, 743–754.

Weber, K., Vollbrecht, A., 1986. Kontinentales Tiefbohrprogramm der Bundesrepublik Deutschland. Ergebnisse der Vorerkundungsarbeiten Lokation Oberpfalz. - 2nd KTB - Kolloquium, Seeheim/Odenwald 19. - 21. Sept. 1986, p. 186.

Wendt, I., Ackermann, H., Carl, C., Kreuzer, H., Müller, P., Stettner, G., 1994. Rb/Sr-Gesamtgesteins- und K/Ar-Glimmerdatierungen der Granite von Flossenbürg und Bärnau. Geol. Jb. E 51, 3–29.

Wise, M.A., 1999. Characterization and classification of NYF-type pegmatites. In The Eugene E. Foord Memorial Symp. on NYF-type Pegmatites (Denver). Can. Mineral. 37, 802–803.
Xiong, X.L., Adam, J., Green, T.H., 2005. Rutile stability and rutile/melt HFSE partitioning during partial melting of hydrous basalt: Implications for TTG genesis. Chem. Geol. 218, 339–359.
Zack, T., von Eynatten, H., Kronz, A., 2004. Rutile geochemistry and its potential use in quantitative provenance studies. Sediment. Geol. 171, 37–58.
Zhovinsky, E. Ya, 1993. Geochemical exploration of ore deposits by the mobile forms of chemical elements. 16th Internation. Geochemical Exploration Symposium, Beijing (China), 1993, p. 48.